HHS Public Access

Author manuscript

Neurobiol Dis. Author manuscript; available in PMC 2018 February 01.

Published in final edited form as:

Neurobiol Dis. 2017 February ; 98: 122–136. doi:10.1016/j.nbd.2016.11.004.

Fbxl18 targets LRRK2 for proteasomal degradation and attenuates cell toxicity

Xiaodong Ding[1], **Sandeep K. Barodia**[2], **Lisha Ma**[1], and **Matthew S. Goldberg**[1,2]

[1]Department of Neurology and Neurotherapeutics, University of Texas Southwestern Medical Center, Dallas, TX, USA

[2]Center for Neurodegeneration and Experimental Therapeutics, Department of Neurology, The University of Alabama at Birmingham, Birmingham, AL, USA

Abstract

Dominantly inherited mutations in leucine-rich repeat kinase 2 (LRRK2) are the most common cause of familial Parkinson's disease (PD) and LRRK2 polymorphisms are associated with increased risk for idiopathic PD. However, the molecular mechanisms by which these mutations cause PD remain uncertain. *In vitro* studies indicate that disease-linked mutations in LRRK2 increase LRRK2 kinase activity and LRRK2-mediated cell toxicity. Identifying LRRK2-interacting proteins and determining their effects on LRRK2 are important for understanding LRRK2 function and for delineating the pathophysiological mechanisms of LRRK2 mutations. Here we identified a novel protein, F-box and leucine-rich repeat domain-containing protein 18 (Fbxl18) that physically associates with LRRK2. We demonstrated that Fbxl18 is a component of a Skp1-Cullin1-F-box ubiquitin ligase complex that regulates the abundance of LRRK2 by selectively targeting phosphorylated LRRK2 for ubiquitination and proteasomal degradation. Knockdown of endogenous Fbxl18 stabilized LRRK2 abundance while protein kinase C activation enhanced LRRK2 degradation by Fbxl18. Dephosphorylation of LRRK2 blocked Fbxl18 association with LRRK2. Taken together, we have identified potential mechanisms for LRRK2 regulation by kinase signaling pathways. Furthermore, Fbxl18 prevented caspase activation and cell death caused by LRRK2 and PD-linked mutant LRRK2. This reveals novel targets for developing potential therapies for familial and idiopathic PD.

INTRODUCTION

Parkinson's disease (PD) is a progressive neurodegenerative movement disorder clinically characterized by bradykinesia, gait disturbances, resting tremor, muscular rigidity, and postural instability. After Alzheimer's disease, PD is the next most common neurodegenerative disease. Some cases of PD (5–10%) are genetically inherited, and

Address correspondence to: Matthew S. Goldberg, Ph.D., Department of Neurology, University of Alabama at Birmingham, 1720 2nd Ave South, Birmingham, AL 35294 USA, Tel: +1-205-934-5228, Fax: +1-205-996-0113, mattgoldberg@uab.edu.

Conflict of Interest Statement: None declared.

mutations in several genes have been causally linked to familial PD (Farrer, 2006; Hardy et al., 2006). Mutations in leucine-rich repeat kinase 2 (LRRK2) are the most common genetic cause of PD and polymorphisms in LRRK2 are associated with increased risk for sporadic PD (Cookson and Bandmann, 2010; Wu et al., 2012; Yue, 2009).

Despite the importance of LRRK2 in PD, the normal cellular function of LRRK2 and pathogenic mechanisms of LRRK2 mutations remain inadequately understood. LRRK2 is a large multi-domain protein consisting of 2527 amino acids with an apparent molecular weight of approximately 285 kDa. LRRK2 contains both active kinase and GTPase domains as well as protein-protein interaction motifs including a leucine-rich repeat (LRR) domain and a WD40 domain (Li et al., 2007; Mata et al., 2006; Webber and West, 2009). *In vitro* studies indicate that disease-linked LRRK2 mutations increase LRRK2 kinase activity and LRRK2-mediated cell toxicity (Greggio et al., 2006; Smith et al., 2006; West et al., 2007). Identifying LRRK2-interacting proteins and determining their effects on LRRK2 are important for understanding LRRK2 function and for delineating the pathophysiological mechanisms of LRRK2 mutations. We and others have identified LRRK2-interacting proteins using a variety of methods, such as yeast two-hybrid screening, co-immunoprecipitation assays and various proteomic approaches (Dachsel et al., 2007; Ding and Goldberg, 2009; Hsu et al., 2010; Ko et al., 2009; Li et al., 2011; Smith et al., 2005; Wang et al., 2008).

Here we report the identification of a novel LRRK2-associated protein, F-box and leucine-rich repeat domain-containing protein 18 (Fbxl18) that binds to LRRK2 and functions as an E3 ubiquitin ligase. Fbxl18 is a member of a family of sixty-eight known human genes encoding F-box motifs (Jin et al., 2004). It has been reported that F-box proteins function as receptors that recruit phosphorylated proteins to Skp1-Cullin1-F-box (SCF) ubiquitin ligase complexes that regulate protein abundance by coupling protein kinase signaling pathways to proteasomal degradation (Cardozo and Pagano, 2004; Lechner et al., 2006; Skowyra et al., 1997). Furthermore, F-box proteins are altered in many diseases, such as cancer and rheumatoid arthritis, and have been proposed as attractive therapeutic targets because of their crucial roles in several important signaling pathways including NF-κB, Wnt and Hedgehog (Jin et al., 2004; Maniatis, 1999).

We found that phosphorylation of LRRK2 was required for Fbxl18 to associate with LRRK2. Protein kinase C mediated phosphorylation of LRRK2 allowed Fbxl18 to bind to LRRK2 and promoted LRRK2 degradation via the ubiquitin proteasome pathway. We discovered that Fbxl18 mitigated cell toxicity caused by PD-linked mutant LRRK2, while knockdown of endogenous Fbxl18 increased LRRK2-mediated cell death, implicating a role for Fbx118 in controlling LRRK2 toxicity. Our results indicate that the Fbxl18 component of the SCF E3 ubiquitin ligase (SCF^{Fbxl18}) regulates LRRK2 abundance and limits LRRK2-mediated cell toxicity by coupling kinase signaling pathways to LRRK2 degradation. These data expand our understanding of the role of SCF complexes and reveal Fbx118 as a novel potential molecular target for developing PD therapies.

RESULTS

Identification of Fbxl18 as a LRRK2 interacting protein

We used each domain of LRRK2 separately as bait to screen a mouse brain cDNA library for protein-protein interactions using yeast two-hybrid analysis. We identified a clone corresponding to the C-terminal portion (amino acids 231–707) of Fbxl18 that interacts with the leucine-rich repeat (LRR) domain of LRRK2 (amino acids 1010–1312). This clone, designated PIP18, includes most of the LRR domain of Fbxl18. We independently validated this interaction in yeast cells using *HIS3* and *ADE1* reporters, and α-gal and β-gal assays (data not shown). To confirm this interaction in mammalian cells, PIP18 and the LRR domain of LRRK2 were respectively subcloned downstream of HA and myc epitope tags in mammalian cell expression vectors (pHA-CMV and pMyc-CMV). Full-length Fbxl18 and full-length LRRK2 were also respectively cloned into pHA-CMV and pMyc-CMV. Co-transfection of HEK293 cells followed by immunoprecipitation (IP) and western blotting showed that the LRR domain of LRRK2 robustly co-immunoprecipitated with PIP18 (Supplemental Figure 1A, right lane). Full-length LRRK2 also co-immunoprecipitated with full-length Fbxl18 (Figure 1, right lane). Interactions were detected by immunoprecipitating myc-tagged LRRK2 and western blotting for the HA-tagged Fbxl18 (Figure 1A) or by immunoprecipitating HA-tagged Fbxl18 and western blotting for the myc-tagged LRRK2 (Figure 1B). Control IPs from cells transfected with equivalent amounts of empty CMV expression vectors (pMyc-CMV or pHA-CMV) confirmed the absence of non-specific binding to the IP antibodies or to the protein A/G beads (Figure 1A and 1B, second from right lanes). Direct western blotting of the cell lysates indicated that the IP results were not due to differences in protein expression levels or transfection efficiencies (Figure 1A and 1B, left two lanes of each panel). Co-expression of Fbxl18 appeared to slightly decrease LRRK2 protein levels. Because PIP18 does not include the N-terminal F-box domain of Fbxl18, this implies that the N-terminal F-box domain of Fbxl18 is dispensable for binding to LRRK2. To verify this, we attempted co-IP from lysates of cells transfected with HA-epitope tagged F-box domain of Fbxl18 and myc-tagged full length LRRK2 and we did not detect any interaction (data not shown). To further confirm the interaction of these two proteins, we performed co-IP of endogenous LRRK2 and Fbxl18 in NIH 3T3 cells using anti-LRRK2 and anti-Fbxl18 antibodies. The physical interaction between endogenous LRRK2 and endogenous Fbxl18 was detected by IP-western analysis using each antibody (Supplemental Figure 1B).

To validate the specificity of the anti-LRRK2 and the anti-Fbxl18 antibodies, we knocked down LRRK2 and Fbxl18 expression in NIH 3T3 cells using specific siRNAs and we observed markedly decreased immunofluorescence signals (Supplemental Figures 2 and 3) consistent with the antibodies being specific for LRRK2 and Fbxl18, respectively. We also confirmed the absence of signal when the primary antibodies were omitted (Supplemental Figure 4). We used the above antibodies to examine the localization of endogenous LRRK2 and endogenous Fbxl18 in NIH 3T3 cells. Confocal microscopy indicates significant co-localization of LRRK2 and Fbxl18 in the cytoplasm (Figure 2). Together, these data demonstrate that Fbxl18 physically and spatially interacts with LRRK2.

Fbxl18 is highly expressed in human cortex and cell lines

Fbxl18 is a novel largely uncharacterized protein. Examination of the primary sequence shows a putative F-box domain near its N-terminus, followed by multiple LRR domains and a putative transmembrane domain near the C-terminus. We examined the expression of Fbxl18 in different cell lines and various human tissues by western analysis using an anti-human Fbxl18 antibody. We detected high levels of Fbxl18 protein in human brain cortex with lower expression in cerebellum and little or no expression in heart, muscle, kidney and spleen (Figure 3). Fbxl18 is also highly expressed in the human neuroblastma SH-SY5Y cell line and at lower levels in the monkey kidney COS7 cell line (Figure 3). Our results demonstrate that Fbxl18 is abundantly expressed in specific tissues and cell lines such as brain and SH-SY5Y cells.

Fbxl18 is a component of an SCF protein complex

F-box proteins comprise a family of homologous proteins sharing a roughly 50 amino acid F-box motif but also have either WD40 repeat domains (short ~40 amino acid motifs, often terminating in Trp-Asp (W-D) dipeptide), LRR domains or various other domains (Jin et al., 2004). The function of many F-box proteins remains unknown, however, they were classically identified as components of a multi-protein complex that catalyzes the ubiquitination of proteins (E3 ubiquitin ligase) and targets specific proteins for degradation by the proteasome (Craig and Tyers, 1999; Kipreos and Pagano, 2000). This type of E3 ubiquitin ligase is often referred to as an SCF complex, named after the three core subunit proteins, S-phase kinase-associated protein 1 (Skp1), Cullin (Cul1) and one of many F-box proteins (Cardozo and Pagano, 2004). The F-box protein interacts with the adaptor Skp1 through its F-box domain. Cul1 functions as a scaffolding protein that binds to both Skp1 and RING finger proteins, such as RING-box protein 1 (Rbx1), that catalyze ubiquitination of substrate proteins that are selectively recruited to the SCF complex by the F-box protein (Cardozo and Pagano, 2004). We found that HEK293 cells express Fbxl18 as well as Skp1 and Cul1, which prompted us to test whether these endogenous proteins form an SCF complex. We used a rabbit anti-Skp1 antibody and a mouse anti-Fbxl18 antibody to immunoprecipitate endogenous Fbxl18 and Skp1 from HEK293 cell lysates. Western blots showed that both Fbxl18 and Skp1 are present in HEK293 cell lysates (Figure 4A, left lanes) and that these two proteins co-immunoprecipitate (Figure 4A, right lane). IgG was used as a negative control to confirm the absence of non-specific binding to the IP antibodies or protein A/G beads. To confirm that the F-box domain is required for Fbxl18 to interact Skp1, lysate from SH-SY5Y cells co-transfected with HA-tagged Fbxl18 lacking its F-box domain (designated as Fbxl18ΔF) and His-tagged Skp1 was used for co-IP. Western blotting results showed that Fbxl18ΔF could not interact with Skp1 in the absence of the F-box domain (Figure 4B). Together, these data imply that Fbxl18 is a component of an SCF complex (SCF^{Fbxl18}) mediated by its F-box domain.

SCF^{Fbxl18} can ubiquitinate LRRK2 and promote LRRK2 degradation through the proteasome pathway

The interactions of LRRK2 with Fbxl18 (Figure 1) and Fbxl18 with Skp1 (Figure 4) prompted us to determine whether Fbxl18 can promote LRRK2 degradation via the

ubiquitin proteasome pathway. Mammalian expression vectors for myc-tagged LRRK2, HA-tagged Fbxl18 and HA-tagged ubiquitin (HA-Ub) were co-transfected into HEK293 cells. After 48 h, cell lysates were immunoprecipitated with anti-myc antibody and ubiquitinated LRRK2 was detected by immunoblotting with anti-ubiquitin antibody (Figure 5, upper panel). Cells transfected with LRRK2 and empty vector (lane 1 from left to right), or pMT-HA-Ub (lane 2) or pHA-Fbxl18 (lane 3) showed little ubiquitination of LRRK2. The faint signal in these cells could be mediated by endogenous Fbxl18 or other E3 ubiquitin ligases. Cells transfected with LRRK2, Fbxl18 and ubiquitin together produced typical high-molecular-weight species consistent with polyubiquitinated LRRK2 (lane 4). Incubation of transfected cells with a proteasome inhibitor, lactacystin, caused the accumulation of polyubiquitinated LRRK2 as determined by the increased intensity of the ubiquitin-immunoreactive smear (lane 5). The same lactacystin treatment of cells transfected with only pMT-HA-Ub and pHA-Fbxl18 (lane 6) showed no signal above background. These results demonstrate the ability of SCF^{Fbxl18} to ubiquitinate LRRK2 and promote LRRK2 degradation via the proteasome.

To further determine the effect of Fbxl18 on the abundance of LRRK2, we co-transfected HEK293 cells with a fixed amount of myc-tagged full-length LRRK2 and increasing amounts of full-length Fbxl18, plus empty vector to normalize all transfections for total DNA. Western analysis of cells harvested 48 h after transfection showed that overexpression of Fbxl18 decreased LRRK2 levels in a dose-dependent manner (Figure 6A). LRRK2 degradation could be attenuated by lactacystin, consistent with Fbxl18 inducing LRRK2 degradation through the proteasome pathway. Blotting with an anti-HA antibody confirmed the increasing amount of Fbxl18 protein in cells transfected with increasing amounts of Fbxl18 expression vector (Figure 6A). ANOVA of densitometry followed by Tukey's multiple comparison test shows that the relative LRRK2 intensity without exogenous Fbxl18 is significantly greater compared to cells transfected with 0.2–1.0 μg of Fbxl18 (Figure 6B). Cells transfected with Fbxl18 in the presence of lactacystin had similar LRRK2 levels compared to cells transfected without Fbxl18, confirming that proteasome activity is required for Fbxl18 to significantly affect LRRK2 levels (Figure 6B). Neither Fbxl18 overexpression nor lactacystin affected the levels of endogenous β-actin (Figure 6A, bottom panel). These data indicate that Fbxl18 can specifically regulate the stability of wild-type LRRK2 by targeting LRRK2 for proteasomal degradation. We also compared the degradation of wild-type and PD-linked mutant LRRK2 (G1441C or G2019S) as well as kinase-dead LRRK2 (D1994A) but we did not observe any differences between wild-type and mutant LRRK2 in Fbxl18-mediated degradation (data not shown).

In parallel with independent studies (Ko et al., 2009), we have previously reported that other proteins, such as the E3 ubiquitin ligase CHIP and heat-shock protein 90, can regulate LRRK2 stability (Ding and Goldberg, 2009). We therefore sought to determine if LRRK2 levels are affected by siRNA-mediated knockdown of endogenous Fbxl18. Because SH-SY5Y cells have a high level of endogenous Fbxl18 (Figure 3), we transfected them with siRNA specific for Fbxl18 or GFP control siRNA together with the myc-LRRK2 expression vector. Western analysis using an anti-Fbxl18 antibody indicated that the Fbxl18 siRNA efficiently knocked down Fbxl18 and stabilized LRRK2 in a dose-dependent manner (Figure 7A). The GFP control siRNA had no effect on the level of Fbxl18 and no effect on the level

of LRRK2 (Figure 7B). To further test for specificity, we co-transfected cells with myc-LRRK2 and another F-box protein, Fbxo7, mutations in which have been causally linked to a parkinsonian-pyramidal syndrome (Di Fonzo et al., 2009). Western analysis showed no effect of Fbxo7 on LRRK2 levels (Supplemental Figure 5). To test the effects of Fbxl18 on physiological levels of LRRK2, we transfected NIH 3T3 cells (which express endogenous LRRK2 and Fbxl18 at levels detectible by direct western analysis) with 10 pmol Fbxl18 siRNA or GFP control siRNA. Western analysis with anti-LRRK2 and anti-Fbxl18 antibodies showed that Fbxl18 siRNA decreased levels of endogenous Fbxl18 and increased levels of endogenous LRRK2 without changing levels of β-actin (Supplemental Figure 6). These results show that siRNA-mediated knockdown of endogenous Fbxl18 increases levels of endogenous LRRK2 and overexpressed LRRK2 in cell lines. To determine if Fbxl18 regulates LRRK2 levels in neurons, we cultured mouse brain striatal neurons and used lentiviral shRNA to knock down endogenous LRRK2 or endogenous Fbxl18. Western analysis showed that GFP control shRNA did not affect the abundance of LRRK2 or Fbxl18, however, Fbxl18 shRNA decreased endogenous Fbxl18 and increased endogenous LRRK2 (Figure 7C and D), indicating that Fbxl18 regulates LRRK2 stability in the neurons. As expected, LRRK2 shRNA specifically decreased endogenous LRRK2 but not Fbxl18 or β-tubulin (Figure 7C and D).

The data thus far suggest that Fbxl18 binds to LRRK2 and targets LRRK2 for proteasomal degradation by recruiting LRRK2 to an SCF complex. The ubiquitination of SCF substrates is mediated by RING finger proteins, such as Rbx1, also known as Roc1 (regulator of Cul1) that bind to the SCF complex via Cul1 (Craig and Tyers, 1999; Kipreos and Pagano, 2000). To verify that Fbxl18-mediated degradation of LRRK2 is dependent on this mechanism, we co-transfected cells to express LRRK2 and Fbxl18 together with a Roc1 silencing vector (psi-Roc1). Western analysis of co-transfected cells shows efficient knockdown of Roc1 protein levels and increasing LRRK2 levels in cells transfected with increasing amounts of psi-Roc1 (Figure 8A). There was little effect of psi-Roc1 on LRRK2 levels in the absence of Fbxl18 co-transfection (Figure 8B) indicating that Roc1 is required but not sufficient for LRRK2 degradation mediated by Fbxl18.

To further characterize Fbxl18 function, we sought to define which portion of Fbxl18 is required for LRRK2 degradation and to determine if any portion is dispensable for this function. We cloned several fragments of Fbxl18 into the pHA-CMV expression vector (pHA-Fbxl18$_{1\text{-}80}$, pHA-Fbxl18$_{1\text{-}300}$, pHA-Fbxl18$_{1\text{-}600}$, pHA-Fbxl18$_{81\text{-}707}$). pHA-Fbxl18$_{1\text{-}80}$ includes only the N-terminal F-box domain. pHA-Fbxl18$_{1\text{-}300}$ and pHA-Fbxl18$_{1\text{-}600}$ include the F-box domain and a few or most of the LRR domains. pHA-Fbxl18$_{81\text{-}707}$ lacks the N-terminal F-box domain. Western analysis of cells co-transfected with myc-LRRK2 and each of these Fbxl18 fragments showed that only the full-length Fbxl18 can efficiently promote LRRK2 degradation, although pHA-Fbxl18$_{1\text{-}600}$ can also slightly promote LRRK2 degradation (Supplemental Figure 7).

Fbxl18-mediated LRRK2 degradation is regulated by protein kinase C

SCF complexes regulate a broad array of cellular signaling pathways by selective proteasomal degradation of substrate proteins via phosphorylation-dependent binding to F-

box proteins (Craig and Tyers, 1999). LRRK2 is known to be phosphorylated and there is an intense effort to map all the sites of LRRK2 phosphorylation and to determine the kinases that phosphorylate LRRK2, in addition to autophosphorylation (Lobbestael et al., 2012; Zhao et al., 2012). We observed that LRRK2 degradation was enhanced by the addition of Ca^{2+} to the culture medium when LRRK2 and Fbxl18 were co-transfected into COS7 cells (Supplemental Figure 8A). In contrast, the intracellular calcium-chelating agent BAPTA-AM blocked Fbxl18-mediated LRRK2 degradation (Supplemental Figure 8B). These observations led us to hypothesize that Ca^{2+}-activated protein kinase C (PKC) was involved in regulating LRRK2 binding to Fbxl18 and subsequent proteasomal degradation. Among the three Ca^{2+} activated PKC isoforms (α, β, γ), only the PKCγ isoform showed the ability to promote LRRK2 degradation in the presence of Fbxl18 (Figure 9). We co-transfected HEK293 cells with myc-tagged LRRK2 and HA-tagged PKCα or PKCβ or PKCγ and we were able to co-IP LRRK2 and PKCγ but not the other PKC isoforms from the cell lysates (Supplemental Figure 9). These results demonstrate that LRRK2 and PKCγ can physically interact, which may promote LRRK2 degradation via Fbxl18. To further test whether PKC activity affects Fbxl18-mediated degradation of LRRK2, we co-transfected cells with LRRK2 and Fbxl18, then treated the cells with either the PKC activator phorbol 12-myristate 13-acetate (PMA) or the PKC inhibitor Go 6983. PMA treatment dosedependently increased LRRK2 degradation (Figure 10A) while Go 6983 had the opposite effect on LRRK2 (Figure 10B). It has been reported that a natural product extracted from green tea (EGCG) is also a PKC activator (Kalfon et al., 2007). We found that EGCG treatment significantly enhanced Fbxl18-mediated LRRK2 degradation in a concentration-dependent manner, similar to PMA (Figure 10C). To verify that the effects of PKC activation and inhibition on LRRK2 are dependent upon Fbxl18, we repeated the above studies on cells co-transfected with LRRK2 but not Fbxl18. In the absence of Fbxl18 co-transfection, PMA, Go 6983, and EGCG treatments showed little to no effect on LRRK2 levels (Supplemental Figure 10).

From these data, we hypothesized that phosphorylation of LRRK2 or its key protein interactors was required for SCF^{Fbxl18} to bind LRRK2 and target LRRK2 for ubiquitin-dependent proteasomal degradation. To test this hypothesis, we co-transfected cells with LRRK2, Fbxl18 and PKCγ. After 24 h, the cells were lysed in the presence of λ-phosphatase to dephosphorylate proteins, or phosphatase inhibitors to preserve protein phosphorylation. We were able to co-IP Fbxl18 and LRRK2 in the presence of phosphatase inhibitors, but dephosphorylation by λ-phosphatase apparently disrupted the physical interaction between LRRK2 and Fbxl18 (Figure 11A and B). Because we initially identified the LRR domain of LRRK2 as the site of interaction with Fbxl18, we speculated that phosphorylation of sites in the LRR domain of LRRK2 are critical for associating with Fbxl18. Parallel IPs from cells co-transfected with the LRR domain of LRRK2 and Fbxl18 revealed that phosphatase inhibitors protected the association of Fbxl18 and LRR domain but λ-phosphatase treatment disrupted their interaction (Figure 11C and D).

Fbxl18 blocks the caspase 8 apoptosis pathway and prevents cell death caused by LRRK2

One of the mechanisms of neuron cell death caused by LRRK2 is the activation of the caspase-8 programmed cell death signaling pathway (Ho et al., 2009). Therefore, caspase-8

can be used as a marker of LRRK2-mediated cytotoxicity. We detected cleaved caspase-8 (41 and 43 kDa bands) in SH-SY5Y cells transfected with LRRK2. However, co-transfection with Fbxl18 decreased LRRK2 western blot density and mitigated caspase-8 cleavage (Figure 12), suggesting that Fbxl18 efficiently blocked the cell death pathway activated by LRRK2. Furthermore, we measured SH-SY5Y cell viability following transfection with wild-type, kinase-dead (D1994A), or PD-linked mutant (G2019S) LRRK2 together with Fbxl18 or empty vector control. G2019S LRRK2 significantly decreased cell viability compared to cells transfected with empty vector or kinase-dead LRRK2 ($p<0.01$), however, co-transfection with Fbxl18 prevented the cell death caused by G2019S LRRK2 (Figure 13A). Moreover, co-transfection with Fbxl18 siRNA significantly increased the cell death caused by G2019S LRRK2 and wild-type LRRK2 (Figure 13B). Fbxl18 siRNA had no effect on the viability of cells co-transfected with kinase-dead LRRK2 or empty vector control. Together, these data confirm that LRRK2 kinase activity is required for LRRK2-mediated cell death and demonstrate that increasing or decreasing Fbxl18 levels can prevent or exacerbate LRRK2-mediated cell death, respectively.

DISCUSSION

PD is the most common neurodegenerative movement disorder and it takes a devastating toll on millions of people. There are currently no treatments proven to slow down the progressive loss of nigral dopamine neurons that underlies the primary clinical symptoms. Despite intensive research, the available medical and surgical therapies are palliative not neuroprotective and PD symptoms invariably get worse as the disease progresses. The lack of more effective therapies is due to the limited understanding of what causes the relatively selective neurodegeneration in PD. Although most cases are idiopathic, about 5–10% of PD cases are caused by inherited genetic mutations. The recent identification of mutations in α-synuclein, LRRK2, Parkin, DJ-1 and PINK1 linked to familial forms of PD provides unprecedented opportunities to identify PD pathogenic mechanisms and to develop more effective therapies based on these pathways (Cookson and Bandmann, 2010; Wu et al., 2012; Yue, 2009). Point mutations in LRRK2 (especially the G2019S mutation) are the most common cause of inherited PD and polymorphisms in LRRK2 are strongly associated with risk for sporadic PD (Cookson and Bandmann, 2010; Wu et al., 2012; Yue, 2009). However, both the normal and the pathophysiological functions of wild-type and mutant LRRK2 are not well understood. Because LRRK2 mutations have been associated with a toxic gain of function (Greggio et al., 2006; Smith et al., 2006; West et al., 2005; West et al., 2007), limiting the cellular amounts of LRRK2 may be both a normal physiological regulatory mechanism for limiting LRRK2-mediated cytotoxicity and a potential PD therapeutic target. Our study advances our understanding of LRRK2 in several important ways.

Cellular levels of LRRK2 are regulated by the ubiquitin proteasome system because inhibition of lysosomal degradation has no effect on LRRK2 while proteasome inhibition causes the accumulation of LRRK2 (West et al., 2005). Mutations in the E3 ubiquitin ligase Parkin (PARK2) have been causally linked to early onset recessive parkinsonism (Kitada et al., 1998). Mutations in Fbxo7 (PARK15), an F-box protein component of an SCF ubiquitin ligase, have been causally linked to a parkinsonism-pyramidal syndrome (Di Fonzo et al., 2009). This genetic data implicates defects in specific components of the ubiquitin

proteasome pathway in the pathogenesis of parkinsonism and related disorders. Our study now provides functional data that another F-box protein, Fbxl18 (but not Fbxo7) directly binds to LRRK2, regulates LRRK2 stability, and controls LRRK2-mediated toxicity. This reveals for the first time an important connection between LRRK2 and SCF-type ubiquitin ligases that bind to substrates via F-box proteins. We show for the first time that Fbxl18 is highly expressed in the brain and neuron-like cell lines such as SH-SY5Y. Like other F-box proteins, Fbxl18 appears to require phosphorylation of substrate proteins in order to bind (Craig and Tyers, 1999; Skowyra et al., 1997). LRRK2 is phosphorylated at a large number of sites, but little is known about the function of LRRK2 phosphorylation (Lobbestael et al., 2012). Here we show that LRRK2 phosphorylation is required for LRRK2 to bind to Fbxl18, and that this interaction is important for regulating the amount of LRRK2 via ubiquitination of LRRK2 by the SCF^{Fbxl18} ubiquitin ligase and subsequent proteasomal degradation of LRRK2. We also show that LRRK2 can induce caspase-8 mediated cell death and that the degradation of LRRK2 mediated by Fbxl18 can prevent LRRK2-mediated toxicity. Together, this suggests that Fbxl18 is an important target to regulate neuronal cell survival and to mitigate LRRK2-mediated cell death *in vitro*. Because LRRK2 mutations cause typical late onset PD with low penetrance, *in vitro* cell death assays may not be physiologically relevant to the mechanisms by which LRRK2 mutations cause disease in humans. Subtle changes in LRRK2 protein levels over many years could eventually manifest in human disease. Although we did not observe any differences between wild-type and PD-linked mutant LRRK2 in Fbxl18-mediated degradation, the effects of the mutations could be too subtle to detect with our methods.

Phosphorylation of LRRK2 at two conserved residues (serine 910 and serine 935) is required for several isoforms of 14-3-3 to bind to LRRK2 and this protein-protein interaction is important for regulating the cytoplasmic localization of LRRK2 and for the secretion of LRRK2 in exosomes (Fraser et al., 2013; Nichols et al., 2010). These sites are just upstream from the LRR fragment of LRRK2 (residues 1010–1312) that we identified as the binding site of Fbxl18. Proteomic studies have identified several serines that are phosphorylated within this segment, including serines 1124, 1253, 1283 and 1292 (Lobbestael et al., 2012) and phosphorylation at other sites may be required for Fbxl18 to bind LRRK2. Some F-box proteins only bind to substrate proteins that are phosphorylated at multiple sites (Nash et al., 2001; Willems et al., 1999). LRRK2 physically interacts with protein kinase C zeta (PKCζ) and is also phosphorylated by PKCζ (Zach et al., 2010). In this study, we found that the gamma isoform of PCK (PKCγ) physically interacts with LRRK2 and can also phosphorylate LRRK2 and promote Fbxl18-mediated LRRK2 degradation. PKCγ is a member of the conventional or typical subgroup of PKC isozymes that are activated by calcium, diacylglycerol and phospholipids. Our data shows LRRK2 degradation is enhanced by overexpression of PKCγ and by application of calcium and the PKC activator PMA but ablated by the PKC inhibitor Go 6983. This provides further evidence that Fbxl18 degrades LRRK2 in a phosphorylation-dependent manner. This is also important because it provides another potential target for PD therapeutics. The green tea polyphenol (-)-epigallocatechin-3-gallate (EGCG) is an activator of protein kinase C (Levites et al., 2002). EGCG has neuroprotective and anti-cancer activities through activation of PKC signaling pathways (Kalfon et al., 2007; Lin, 2002). A proteomics

analysis identified induction of PKC by EGCG in a progressive model of neuronal death (Weinreb et al., 2008). More recent studies showed EGCG can restore the neuronal loss and molecular targets damaged in animal models of parkinsonism (Reznichenko et al., 2010). EGCG can prevent neuronal cell toxicity induced by overexpressing the A53T mutant form of α-synuclein linked to PD and can prevent PD-related pathology induced by 6-hydroxydopamine in PD animal models (Chao et al., 2010; Ma et al., 2010). We now show a mechanism whereby EGCG negatively regulates LRRK2 stability in cells. Taken together, our data shows evidence of a novel and important LRRK2 interacting protein that integrates cell signaling pathways, regulates LRRK2 stability, mitigates LRRK2-mediated cell toxicity and provides additional potential targets for PD therapeutics.

MATERIALS AND METHODS

Plasmid constructs and lentiviral particles

RNA was isolated from mouse brains, reverse transcribed and used for PCR amplification of LRRK2 and Fbxl18 cDNA. Full-length LRRK2 cDNA was cloned into pMyc-CMV (Clontech) for mammalian cell transfections and expression of myc-epitope tagged LRRK2. LRRK2 point mutations (G2019S, G1441C and D1994A) were generated using the QuickChange Site-Directed Mutagenesis kit (Stratagene). Full-length Fbxl18 cDNA was cloned into pHA-CMV (Clontech) for expression of HA-epitope tagged Fbxl18. Individual LRRK2 domains comprising amino acids 1–690 (ARM), 691–1009 (Ankyrin), 1010–1312 (LRR), 1331–1512 (ROC), 1514–1866 (COR), 1869–2128 (kinase) and 2141–2432 (WD40) were subcloned into pGBKT7 (Clontech) for yeast two-hybrid analyses. psi-Roc1 was kindly provided by Dr. Yi Sun. pHis-Roc1 was kindly provided by Dr. Michele Pagano. pMT-HA-Ub was kindly provided by Dr. Pat Gallagher. Full-length human Fbxo7 was purchased from Origene, Inc. Lentiviral particles to express GFP (sc-108084), LRRK2 shRNA (sc-45750-V) and Fbxl18 shRNA (sc-145092-V) were purchased from Santa Cruz.

Antibodies and other reagents

The following antibodies and other reagents were used in these studies: Mouse monoclonal anti-Fbxl18 (#ab57768-100 Abcam, Cambridge, MA); Mouse monoclonal anti-HA (#MMS-101P Covance, Emeryville, CA); Mouse monoclonal anti-myc (#GTX20032 GeneTex, San Antonio, TX); Rabbit anti-HA (#ab9110 Abcam, Cambridge, MA); Rabbit anti-myc (#2272) and mouse monoclonal anti-His (#2366) (Cell Signaling Technology, Danvers, MA); Mouse anti-β-actin (#AAN02 Cytoskeleton, Denver, CO); Mouse anti-ubiquitin (#13-1600, Invitrogen); Rabbit anti-Roc1, rabbit anti-Skp1 and rabbit anti-Cul1 antibodies were obtained from the laboratory of Dr. Yue Xiong at the University of North Carolina. Alexa Fluor® 488 FluoroNanogold Fab' fragment of goat anti-rabbit IgG (cat no: A24922) and Alexa Fluor® 594 FluoroNanogold Fab' fragment of goat anti-mouse IgG (can no: A24921) were purchased from Invitrogen. Rabbit IgG, Peroxidase-conjugated goat anti-mouse IgG(H+L) and anti-rabbit IgG(H+L) were purchased from Jackson ImmunoResearch Laboratories. Rabbit monoclonal anti-LRRK2 (clone ID MJFF3[c69-6]) was provided by the Michael J. Fox Foundation for Parkinson's Research. (-)-Epigallocatechin gallate (#270-263-M010) and BAPTA-AM (#450-014-M010) were purchased from Alexis (San Diego, CA). Phorbol-12-myristate-13-acetate (524400) and Go6983 (365251) were

purchased from Calbiochem (Darmstadt, Germany). Fbxl18 siRNA (sc-89395) and control siRNA (sc-36869) were purchased from Santa Cruz (Santa Cruz, CA). Lipofectamine 2000 (11668-027) was purchased from Invitrogen (Carlsbad, CA). Complete protease inhibitor cocktail (11873580001) was purchased from Roche Molecular Biochemicals (Indianapolis, IN). Lactacystin (70980) was purchased from Cayman Chemical (Ann Arbor, MI). ImmunoPure Immobilized Protein A/G beads (20421) were purchased from Pierce (Rockford, IL). X-α-Gal was purchased from Growcells (Irvine, CA). X-β-Gal was purchased from Zymo Research (Orange, CA). Yeast nitrogen base w/o amino acids (291940) and amino acid Drop-out supplements (DO-Leu, DO-Trp, DO-Leu-Trp, DO-Leu-Trp-His, DO-Leu-Trp-His-Ade) were from Clontech. 3-AT (3-amino-1,2,4-triazole) and cycloheximide (#01810) were purchased from Sigma. ToxCount Cell Viability Assay kit was purchase from Active Motif (Carlsbad, CA). Human brain samples (cerebellum and cortex) were kindly provided by Dr. Charles White. The other tissues (muscle, kidney, heart and spleen) were obtained from the University of Texas Southwestern Medical Center Tissue Resource Center.

Yeast Two-Hybrid Analyses

Bait plasmids consisting of each individual LRRK2 domain in pGBKT7 (Clontech) were transformed into yeast strain AH109 (*MATa, trp1-901, leu2-3, 112, ura3-52, his3-200, gal4*Δ, *gal80*Δ, *LYS2: :GAL1*$_{UAS}$*-GAL1*$_{TATA}$*-HIS3, GAL2*$_{UAS}$*-GAL2*$_{TATA}$*-ADE2, URA3: :MEL1*$_{UAS}$*-MEL1*$_{TATA}$*-lacZ*) (Clontech). Yeast clones harboring the bait plasmids were selected on SD/-Trp medium. Bait autoactivation was tested on SD/-Trp-His medium. Baits with little or no autoactivation were used to screen a mouse brain cDNA library (Clontech catalog number 638863) pre-transformed in yeast strain Y187 (*MAT*α, *ura3-52*, *his3-200, ade2-101*, *trp1-901, leu2-3, 112, gal4Δ, met–, gal80Δ, URA3: :GAL1*$_{UAS}$*-GAL1*$_{TATA}$*-lacZ*) (Clontech). Yeast two-hybrid screens were performed as previously described (Ding and Goldberg, 2009) using the Matchmaker GAL4 system (Clontech). Briefly, AH109 yeast cells harboring one bait plasmid were mated with Y187 cells harboring the Clontech Matchmaker mouse brain cDNA library. The diploid zygotes (5×10^6) were plated on triple selective medium (SD/-Leu-Trp-His plus 5 mM 3-AT). The prey plasmids from yeast colonies growing on the triple selective medium were rescued and sequenced. To further verify the interactions in yeast cells, the obtained prey plasmids and their bait plasmid were co-transformed into AH109 yeast cells. After growing up on double selective medium (SD/-Trp-Leu), the yeast cells were re-streaked onto quadruple selective medium (SD/-Leu-Trp-His-Ade plus 2 mM 3-AT) and were used to perform X-α-Gal assays (*MEL1* reporter) and X-β-Gal colony-lift assays (*LacZ* reporter) according to the Yeast Protocols Handbook (Clontech).

Cell Growth and Transfection

HEK293 cells were maintained in DMEM with 4 mM L-glutamine, 4.5g/liter glucose, 10% FBS, 50 U penicillin, 50 μg/ml streptomycin. Neuroblastoma SH-SY5Y cells were maintained in DMEM/F12 (1:1) medium with 10% FBS and 50 U penicillin, 50 μg/ml streptomycin. For HEK293 cell transfection, cells (80% confluence) were transfected with an equal amount of total plasmid DNA (adjusted with the corresponding empty vector) by the calcium phosphate method. For siRNA transfection into NIH 3T3 cells, 40–50%

confluent cells were transfected with 0–40 picomoles of Fbxl18 siRNA or control siRNA using Lipofectamine 2000 or RNAiMAX cell transfection reagent according to the manufacturer's instructions. Mouse brain striatum neuron cells were purchased from Thermo Fisher (M-CP-302) and were grown in neurobasal-A medium (21103-049, Gibco) plus 0.5 mM L-glutamine and 1× B-27 supplement (17504-044, Gibco) without serum for 2–3 days, then transfected with lentivirus.

Co-localization and Confocal Microscopy

Cultured NIH 3T3 cells (which express endogenous LRRK2 and Fbxl18) were fixed in 4% paraformaldehyde for 20 min and permeabilized with 0.5% Triton X-100 in CWFS buffer (1.35% cold water fish skin in TBS buffer (p7.4)) for 15 min then blocked in CWFS buffer for 15 min at room temperature. The cells were incubated with primary antibodies (Abcam ab57768 mouse anti-Fbxl18 and c69-6 rabbit anti-LRRK2) in CWFS buffer with 0.1% Triton X-100 followed by fluorophore-conjugated secondary antibodies (Alexa Fluor® 488 anti-rabbit IgG and Alexa Fluor® 594 anti-mouse IgG). Cells were stained with DAPI to visualize nuclei. Primary antibody specificity was validated by immunofluorescence of NIH 3T3 cells with and without specific siRNAs to knock down target protein expression (Supplemental Figures 2 and 3). Cells stained with only secondary antibody (no primary antibody) were used to validate the specificity of the secondary antibodies (Supplemental Figure 4). Confocal images were acquired and analyzed for protein co-localization using Zeiss 510 and Leica TCS SP5 confocal microscopes.

Immunoprecipitation and Western blot

48 h after transfection, cells were lysed in 500 μl ice-cold buffer (50 mM Tris pH 7.4, 150 mM NaCl, 1% NP-40, 1× Roche complete protease inhibitor cocktail). Cell lysates were incubated on ice for 30 min and centrifuged at 12,000*g* for 10 min at 4°C. Equal amounts of total protein from the supernatants were pre-cleared at 4°C for 1 h with 10 μl of ImmunoPure Immobilized Protein A/G beads. Rabbit polyclonal antibody (anti-myc or anti-HA) was added to the pre-cleared supernatants at 1:500 dilution and incubated at 4°C for 2 h. 20 μl of ImmunoPure Immobilized Protein A/G beads was added and incubated for another 1 h. The beads were washed five times in ice-cold lysis buffer with 1× protease inhibitor cocktail. Proteins were eluted from the beads by heating at 95°C in 1× Laemmli buffer, resolved on 4–20% gradient gels (BioRad), transferred to nitrocellulose and detected by western blot using mouse monoclonal anti-HA or anti-myc antibodies, HRP-conjugated goat anti-mouse secondary antibodies (Jackson Immunoresearch) and chemiluminescent detection (Pierce).

Ubiquitination Assay

pMyc-LRRK2, pHA-Fbxl18 and pMT-HA-Ub were co-transfected into HEK293 cells. After incubation for 48 h, IP was performed using anti-myc antibody (Cell Signaling #2276S). Anti-ubiquitin antibody (sc8017) was used to detect the ubiquitination of LRRK2. Anti-myc antibody was also used to probe total lysates for LRRK2 expression and to probe immunoprecipitants to confirm LRRK2 pulldown efficiency and specificity.

Cell viability and cell death assay

Neuroblastoma SH-SY5Y cells were co-transfected with the indicated DNA constructs or siRNA in 96-well format. After 48 h at 37°C (5% CO2), cells were briefly washed with PBS. 50 μl of PBS containing calcein-AM and EthD-1 were added to each well according to the ToxCount manual and the cells were incubated for 30 minutes at 37°C. The number of live and dead cells was measured using an Isocyte automated cell scanner (Blueshift Biotechnologies, Sunnyvale, CA) according to the manufacturer's instructions.

Supplementary Material

Refer to Web version on PubMed Central for supplementary material.

Acknowledgments

We thank Marian Marvin for cloning mouse LRRK2 cDNA and assistance with site-directed mutagenesis. We thank Joseph Albanesi and Charlene Supnet for critical reading and comments on the manuscript.

FUNDING

This work was supported by the National Institute of Neurological Disorders and Stroke grant number R21NS072754, the Michael J. Fox Foundation for Parkinson's Research, the David M. Crowley Foundation, and Parkinson's Benefactors.

REFERENCES

Cardozo T, Pagano M. The SCF ubiquitin ligase: insights into a molecular machine. Nat Rev Mol Cell Biol. 2004; 5:739–751. [PubMed: 15340381]

Chao J, et al. A pro-drug of the green tea polyphenol (-)-epigallocatechin-3-gallate (EGCG) prevents differentiated SH-SY5Y cells from toxicity induced by 6-hydroxydopamine. Neurosci Lett. 2010; 469:360–364. [PubMed: 20026175]

Cookson MR, Bandmann O. Parkinson's disease: insights from pathways. Hum Mol Genet. 2010; 19:R21–R27. [PubMed: 20421364]

Craig KL, Tyers M. The F-box: a new motif for ubiquitin dependent proteolysis in cell cycle regulation and signal transduction. Prog Biophys Mol Biol. 1999; 72:299–328. [PubMed: 10581972]

Dachsel JC, et al. Identification of potential protein interactors of Lrrk2. Parkinsonism Relat Disord. 2007; 13:382–385. [PubMed: 17400507]

Di Fonzo A, et al. FBXO7 mutations cause autosomal recessive, early-onset parkinsonian-pyramidal syndrome. Neurology. 2009; 72:240–245. [PubMed: 19038853]

Ding X, Goldberg MS. Regulation of LRRK2 stability by the E3 ubiquitin ligase CHIP. PLoS One. 2009; 4:e5949. [PubMed: 19536328]

Farrer MJ. Genetics of Parkinson disease: paradigm shifts and future prospects. Nat Rev Genet. 2006; 7:306–318. [PubMed: 16543934]

Fraser KB, et al. LRRK2 secretion in exosomes is regulated by 14-3-3. Hum Mol Genet. 2013; 22:4988–5000. [PubMed: 23886663]

Greggio E, et al. Kinase activity is required for the toxic effects of mutant LRRK2/dardarin. Neurobiol Dis. 2006; 23:329–341. [PubMed: 16750377]

Hardy J, et al. Genetics of Parkinson's disease and parkinsonism. Ann Neurol. 2006; 60:389–398. [PubMed: 17068789]

Ho CC, et al. The Parkinson disease protein leucine-rich repeat kinase 2 transduces death signals via Fas-associated protein with death domain and caspase-8 in a cellular model of neurodegeneration. J Neurosci. 2009; 29:1011–1016. [PubMed: 19176810]

Hsu CH, et al. MKK6 binds and regulates expression of Parkinson's disease-related protein LRRK2. J Neurochem. 2010; 112:1593–1604. [PubMed: 20067578]

Jin J, et al. Systematic analysis and nomenclature of mammalian F-box proteins. Genes Dev. 2004; 18:2573–2580. [PubMed: 15520277]

Kalfon L, et al. Green tea polyphenol (-)-epigallocatechin-3-gallate promotes the rapid protein kinase C- and proteasome-mediated degradation of Bad: implications for neuroprotection. J Neurochem. 2007; 100:992–1002. [PubMed: 17156130]

Kipreos ET, Pagano M. The F-box protein family. Genome Biol. 2000; 1 REVIEWS3002.

Kitada T, et al. Mutations in the parkin gene cause autosomal recessive juvenile parkinsonism. Nature. 1998; 392:605–608. [PubMed: 9560156]

Ko HS, et al. CHIP regulates leucine-rich repeat kinase-2 ubiquitination, degradation, and toxicity. Proc Natl Acad Sci U S A. 2009; 106:2897–2902. [PubMed: 19196961]

Lechner E, et al. F-box proteins everywhere. Curr Opin Plant Biol. 2006; 9:631–638. [PubMed: 17005440]

Levites Y, et al. Involvement of protein kinase C activation and cell survival/ cell cycle genes in green tea polyphenol (-)-epigallocatechin 3-gallate neuroprotective action. J Biol Chem. 2002; 277:30574–30580. [PubMed: 12058035]

Li X, et al. Leucine-rich repeat kinase 2 (LRRK2)/PARK8 possesses GTPase activity that is altered in familial Parkinson's disease R1441C/G mutants. J Neurochem. 2007; 103:238–247. [PubMed: 17623048]

Li X, et al. Phosphorylation-dependent 14-3-3 binding to LRRK2 is impaired by common mutations of familial Parkinson's disease. PLoS ONE. 2011; 6:e17153. [PubMed: 21390248]

Lin JK. Cancer chemoprevention by tea polyphenols through modulating signal transduction pathways. Arch Pharm Res. 2002; 25:561–571. [PubMed: 12433185]

Lobbestael E, et al. Phosphorylation of LRRK2: from kinase to substrate. Biochem Soc Trans. 2012; 40:1102–1110. [PubMed: 22988873]

Ma L, et al. Genome-wide microarray analysis of the differential neuroprotective effects of antioxidants in neuroblastoma cells overexpressing the familial Parkinson's disease alpha-synuclein A53T mutation. Neurochem Res. 2010; 35:130–142. [PubMed: 19649707]

Maniatis T. A ubiquitin ligase complex essential for the NF-kappaB, Wnt/Wingless, and Hedgehog signaling pathways. Genes Dev. 1999; 13:505–510. [PubMed: 10072378]

Mata IF, et al. LRRK2 in Parkinson's disease: protein domains and functional insights. Trends Neurosci. 2006

Nash P, et al. Multisite phosphorylation of a CDK inhibitor sets a threshold for the onset of DNA replication. Nature. 2001; 414:514–521. [PubMed: 11734846]

Nichols RJ, et al. 14-3-3 binding to LRRK2 is disrupted by multiple Parkinson's disease-associated mutations and regulates cytoplasmic localization. Biochem J. 2010; 430:393–404. [PubMed: 20642453]

Reznichenko L, et al. Low dosage of rasagiline and epigallocatechin gallate synergistically restored the nigrostriatal axis in MPTP-induced parkinsonism. Neurodegener Dis. 2010; 7:219–231. [PubMed: 20197647]

Skowyra D, et al. F-box proteins are receptors that recruit phosphorylated substrates to the SCF ubiquitin-ligase complex. Cell. 1997; 91:209–219. [PubMed: 9346238]

Smith WW, et al. Kinase activity of mutant LRRK2 mediates neuronal toxicity. Nat Neurosci. 2006; 9:1231–1233. [PubMed: 16980962]

Smith WW, et al. Leucine-rich repeat kinase 2 (LRRK2) interacts with parkin, and mutant LRRK2 induces neuronal degeneration. Proc Natl Acad Sci U S A. 2005; 102:18676–10681. [PubMed: 16352719]

Wang L, et al. The chaperone activity of heat shock protein 90 is critical for maintaining the stability of leucine-rich repeat kinase 2. J Neurosci. 2008; 28:3384–3391. [PubMed: 18367605]

Webber PJ, West AB. LRRK2 in Parkinson's disease: function in cells and neurodegeneration. Febs J. 2009; 276:6436–6444. [PubMed: 19804415]

Weinreb O, et al. The application of proteomics for studying the neurorescue activity of the polyphenol (-)-epigallocatechin-3-gallate. Arch Biochem Biophys. 2008; 476:152–160. [PubMed: 18211800]

West AB, et al. Parkinson's disease-associated mutations in leucine-rich repeat kinase 2 augment kinase activity. Proc Natl Acad Sci U S A. 2005; 102:16842–16847. [PubMed: 16269541]

West AB, et al. Parkinson's disease-associated mutations in LRRK2 link enhanced GTP-binding and kinase activities to neuronal toxicity. Hum Mol Genet. 2007; 16:223–232. [PubMed: 17200152]

Willems AR, et al. SCF ubiquitin protein ligases and phosphorylation-dependent proteolysis. Philos Trans R Soc Lond B Biol Sci. 1999; 354:1533–1550. [PubMed: 10582239]

Wu X, et al. Quantitative assessment of the effect of LRRK2 exonic variants on the risk of Parkinson's disease: a meta-analysis. Parkinsonism Relat Disord. 2012; 18:722–730. [PubMed: 22575234]

Yue Z. LRRK2 in Parkinson's disease: in vivo models and approaches for understanding pathogenic roles. Febs. J. 2009; 276:6445–6454. [PubMed: 19804414]

Zach S, et al. Signal transduction protein array analysis links LRRK2 to Ste20 kinases and PKC zeta that modulate neuronal plasticity. PLoS ONE. 2010; 5:e13191. [PubMed: 20949042]

Zhao J, et al. Pharmacological inhibition of LRRK2 cellular phosphorylation sites provides insight into LRRK2 biology. Biochem Soc Trans. 2012; 40:1158–1162. [PubMed: 22988882]

Highlights

We identified a novel protein, Fbxl18, that associates with LRRK2 and targets LRRK2 for degradation by the proteasome.

We demonstrate that phosphorylation of LRRK2 is required for Fbxl18 to bind to LRRK2 and to promote LRRK2 degradation.

We show that siRNA-mediated knockdown of endogenous Fbxl18 increases levels of endogenous LRRK2 while overexpression of Fbxl18 decreases LRRK2 levels.

Increasing or decreasing Fbxl18 mitigates or enhances LRRK2-mediated cell toxicity.

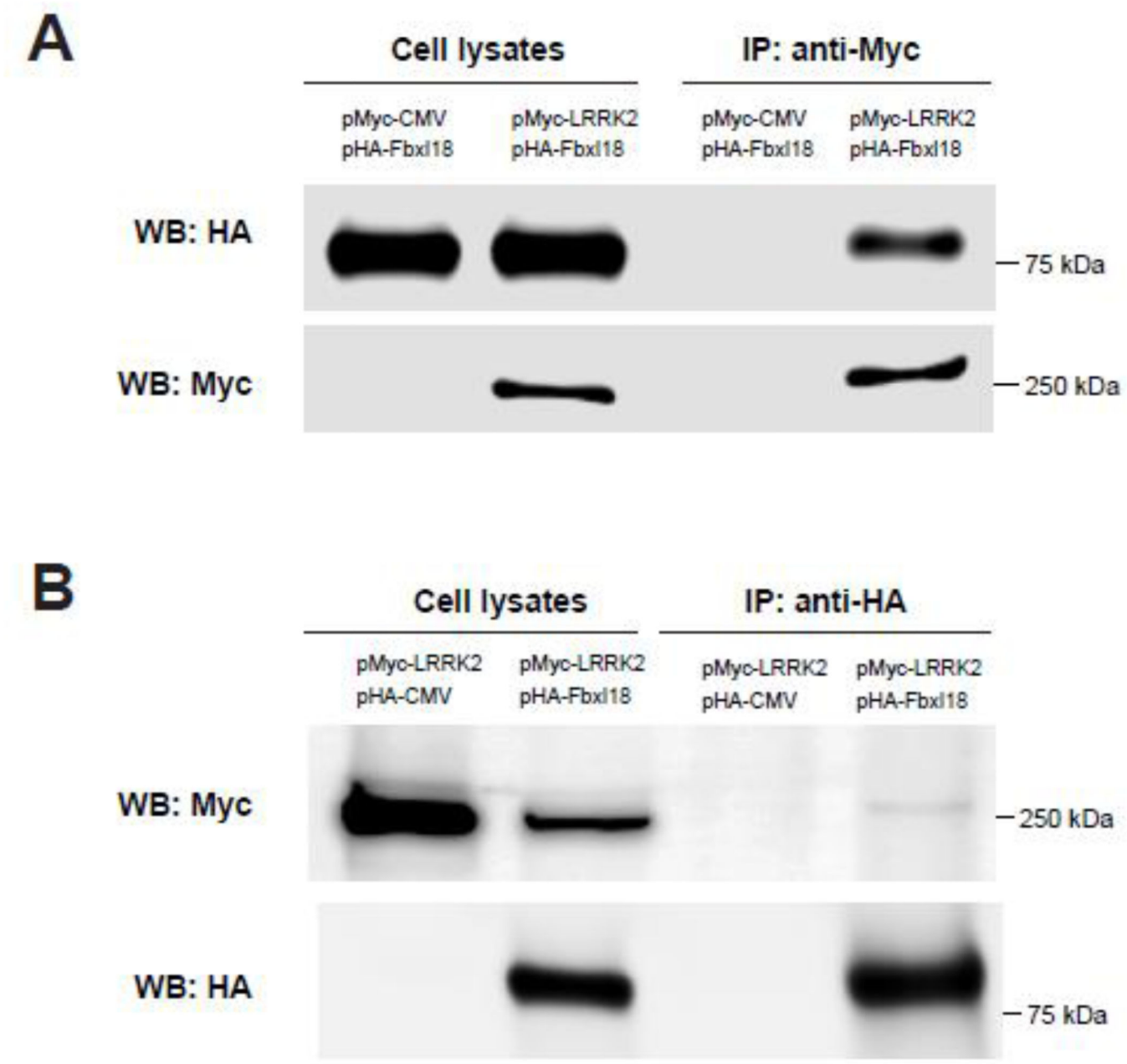

Figure 1.

Physical interaction of Fbxl18 and LRRK2. (A) HEK293 cells were co-transfected with pHA-Fbxl18 and pMyc-LRRK2 or pMyc-CMV control and the cell lysates were immunoprecipitated using an anti-myc antibody. Total cell lysates (left two lanes) and immunoprecipitants (right two lanes) were immunoblotted using an anti-HA antibody (upper panel) to confirm similar expression and to detect co-immunoprecipitation. Total cell lysates and immunoprecipitants were also immunoblotted using anti-myc antibody (lower panel) to confirm LRRK2 pulldown efficiency and specificity. (B) HEK293 cells were co-transfected with pMyc-LRRK2 and either pHA-Fbxl18 or pHA-CMV control and the cell lysates were immunoprecipitated using anti-HA antibody. Total cell lysates (left two lanes) and

immunoprecipitants (right two lanes) were immunoblotted using an anti-myc antibody to detect co-immunoprecipitation (upper panel) and also immunoblotted using anti-HA antibody (lower panel) to confirm Fbxl18 pulldown efficiency and specificity. Equal amounts of total protein (2 μg) were loaded in cell lysate lanes. 200 μg of cell lysate was used for immunoprecipitation and 20% of the eluate was loaded in the IP lanes.

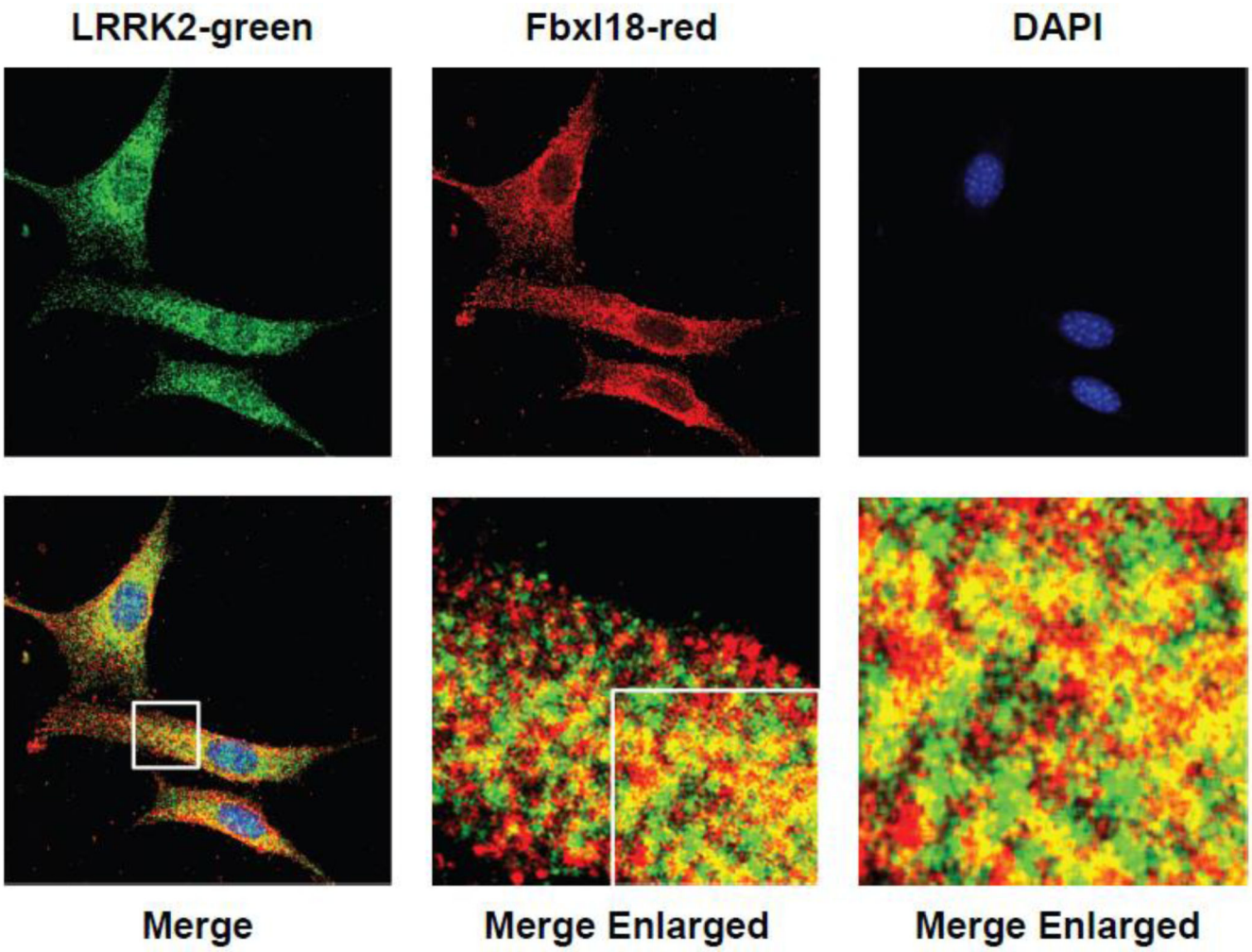

Figure 2.

Co-localization of endogenous LRRK2 and endogenous Fbxl18. NIH 3T3 cells were fixed and immunostained with anti-LRRK2 and anti-Fbxl18 primary antibodies, followed by Alexa-488 and -594 secondary antibodies, respectively. Cell nuclei were stained with DAPI. The cells were imaged by confocal microscopy. The green channel for LRRK2, the red channel for Fbxl18, and blue channel for nuclei are shown individually on top. The bottom row shows the merged images of all three channels and high magnification images of the boxed area to show the partial co-localization of the LRRK2 and Fbxl18 signals in the cytoplasm.

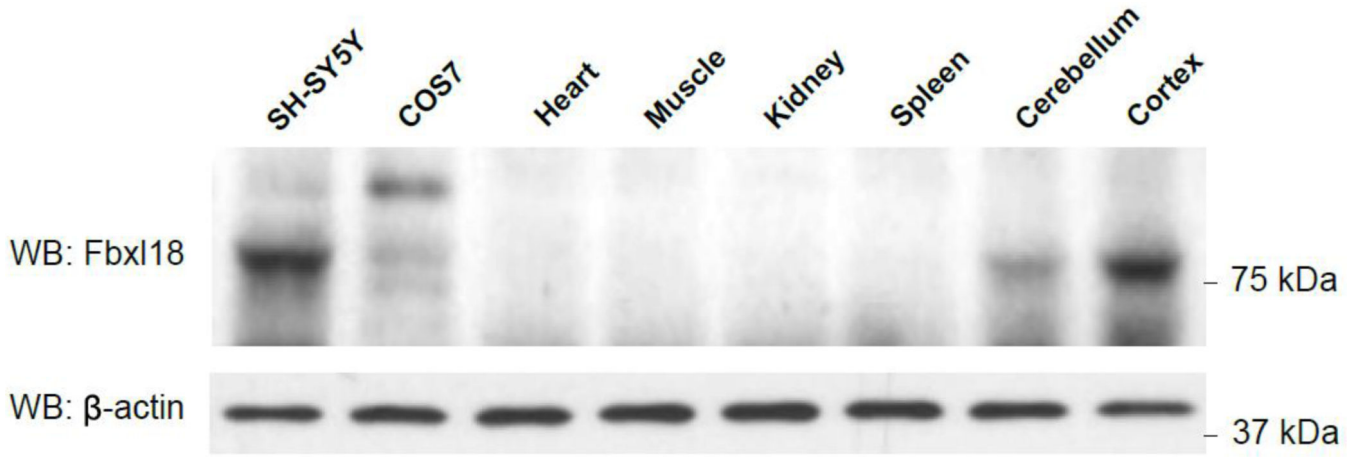

Figure 3.

Fbxl18 expression in different cell lines and human tissues. Proteins were extracted from cell lines and various human tissues by homogenization in RIPA buffer (10 mM Tris pH 8.0, 1 mM EDTA, 0.5 mM EGTD, 1% Triton X-100, 0.1% SDS, 140 mM NaCl) with protease inhibitors. Following brief centrifugation, 5 μg of total protein from cleared cell lysates or tissue homogenates was loaded in each lane and resolved by 10% SDS-PAGE. The membrane was blotted with an anti-Fbxl18 antibody and re-probed with anti-β-actin antibody to confirm similar loading of each lane. Extracts were loaded in the indicated lanes 1: SH-SY5Y cells; 2: COS7 cells; 3: heart; 4; muscle; 5: kidney; 6: spleen; 7: cerebellum; 8: cerebral cortex.

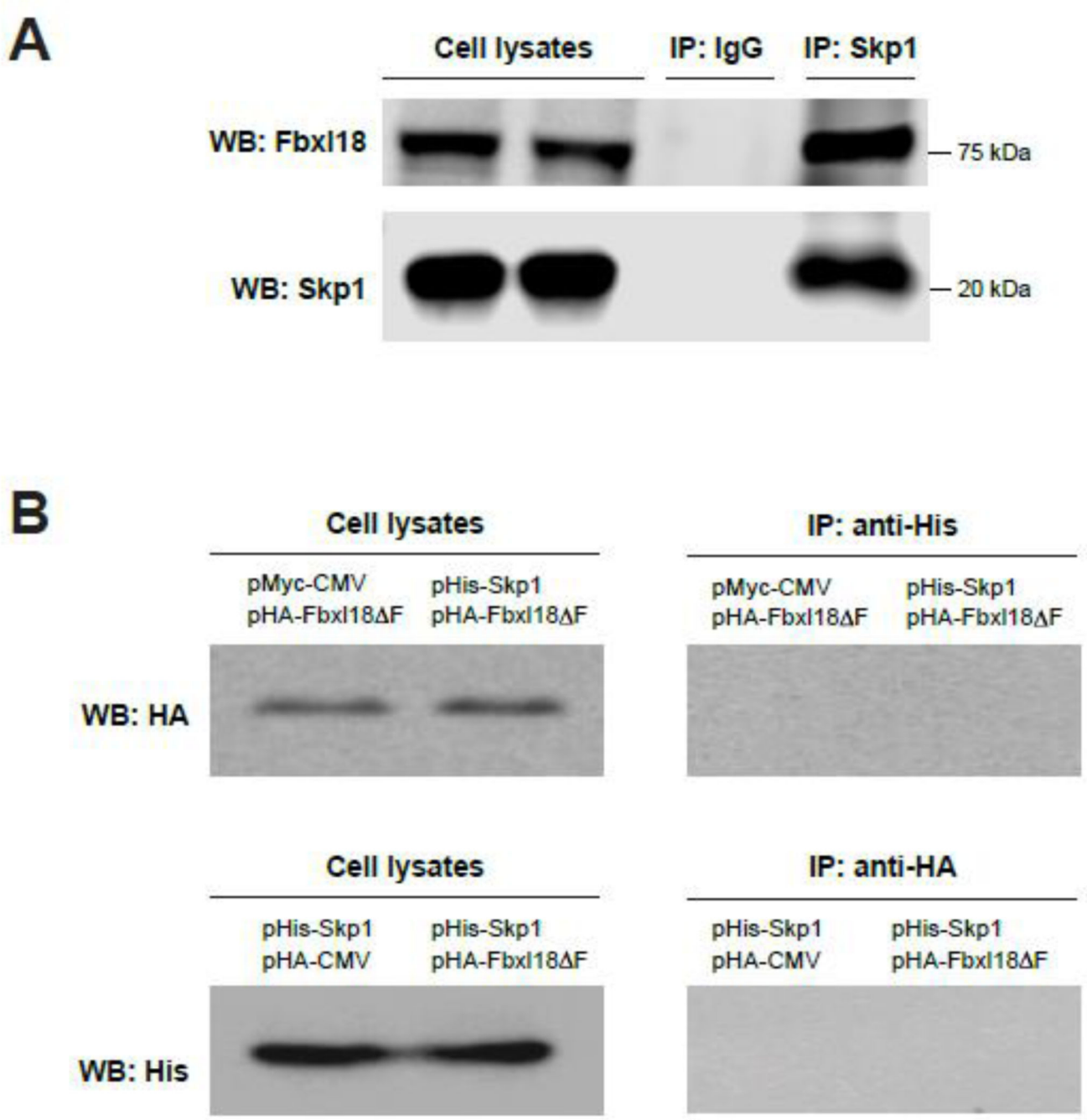

Figure 4.

(A) Association of Fbxl18 and Skp1. Total cell lysates and anti-Skp1 immunoprecipitates from untransfected HEK293 cells were western blotted with anti-Fbxl18 antibody (upper panel) to confirm similar protein levels and to detect co-immunoprecipitation of endogenous Skp1 and endogenous Fbxl18. The same samples were also western blotted with anti-Skp1 (lower panel) to show Skp1 pulldown efficiency and specificity. IgG was used as a negative control for IP. Equal amounts of total protein (2 μg) were loaded in cell lysate lanes. 500 μg of cell lysate was used for immunoprecipitation and 20% of the eluate was loaded in the IP

lanes. (B) Deletion of F-box domain of Fbxl18 abolishes the interaction of Fbxl18 and Skp1. SH-SY5Y cells were co-transfected with HA-tagged Fbxl18ΔF (Fbxl18 lacking the F-box domain) and His-tagged Skp1 or empty vector control (pMyc-CMV). Total cell lysates (left panel) and anti-His immunoprecipitants (right panel) were immunoblotted using an anti-HA antibody (upper panels). In parallel, total cell lysates (left panel) and anti-HA immunoprecipitants (right panel) were immunoblotted using an anti-His antibody (lower panels).

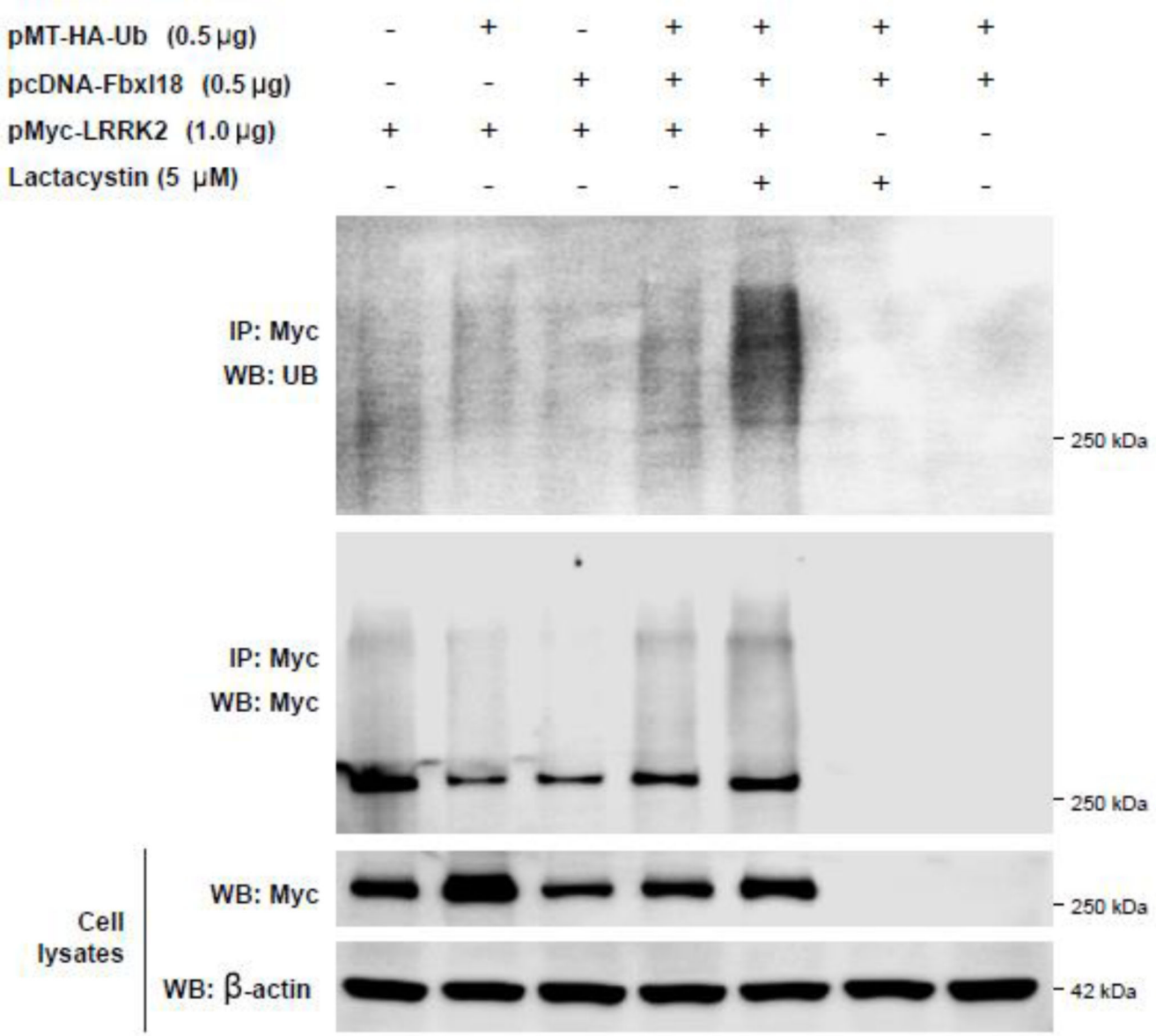

Figure 5.

Fbxl18 promotes LRRK2 ubiquitination. HEK293 cells were transfected with the indicated DNA constructs and treated with lactacystin or vehicle as indicated. The cell lysates were immunoprecipitated using an anti-myc antibody and western blotted with anti-ubiquitin (upper panel) and anti-myc (second panel) to reveal LRRK2 ubiquitination relative to LRRK2 pulldown efficiency. 500 µg of cell lysate was used for immunoprecipitation and 40% of the eluate was loaded in the IP lanes. 5 µg of total cell lysate protein per lane was analyzed by western blot with anti-myc (third panel) and anti-β-actin (bottom panel) to show relative levels of LRRK2 protein in the cell lysates used for IP.

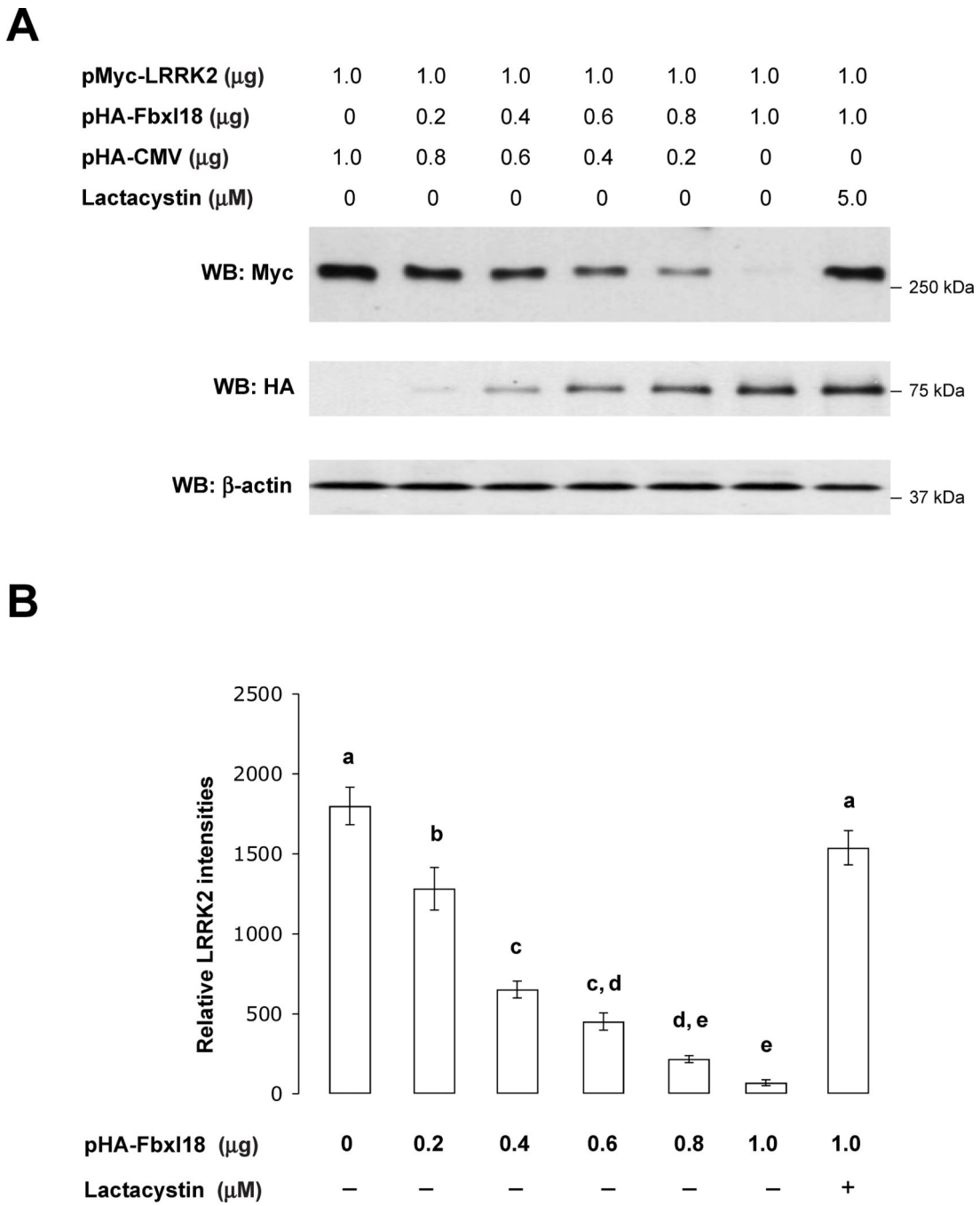

Figure 6.

Fbxl18 can ubiquitinate LRRK2 and promote LRRK2 degradation through the proteasome pathway. (A) HEK293 cells were co-transfected with 1.0 μg of pMyc-LRRK2 and 0, 0.2, 0.4, 0.6, 0.8 or 1.0 μg of pHA-Fbxl18 as indicated. The empty vector pHA-CMV was used to make equal the total amount of DNA used for each transfection. The proteasome inhibitor, lactacystin, was added to the cell culture at a final concentration of 0 or 5 μM, as indicated. After 48 h, cell lysates were analyzed by western blotting with anti-myc (upper), anti-HA (middle) or anti-β-actin (lower panel). (B) Densitometry was used to measure LRRK2 levels

in (A). Bar graph shows mean LRRK2 intensity (N = 3) and error bars show +/− SEM. Columns with the same letter above them are not significantly different whereas columns with different letters are significantly different according to ANOVA followed by Tukey's multiple comparisons test ($p<0.05$).

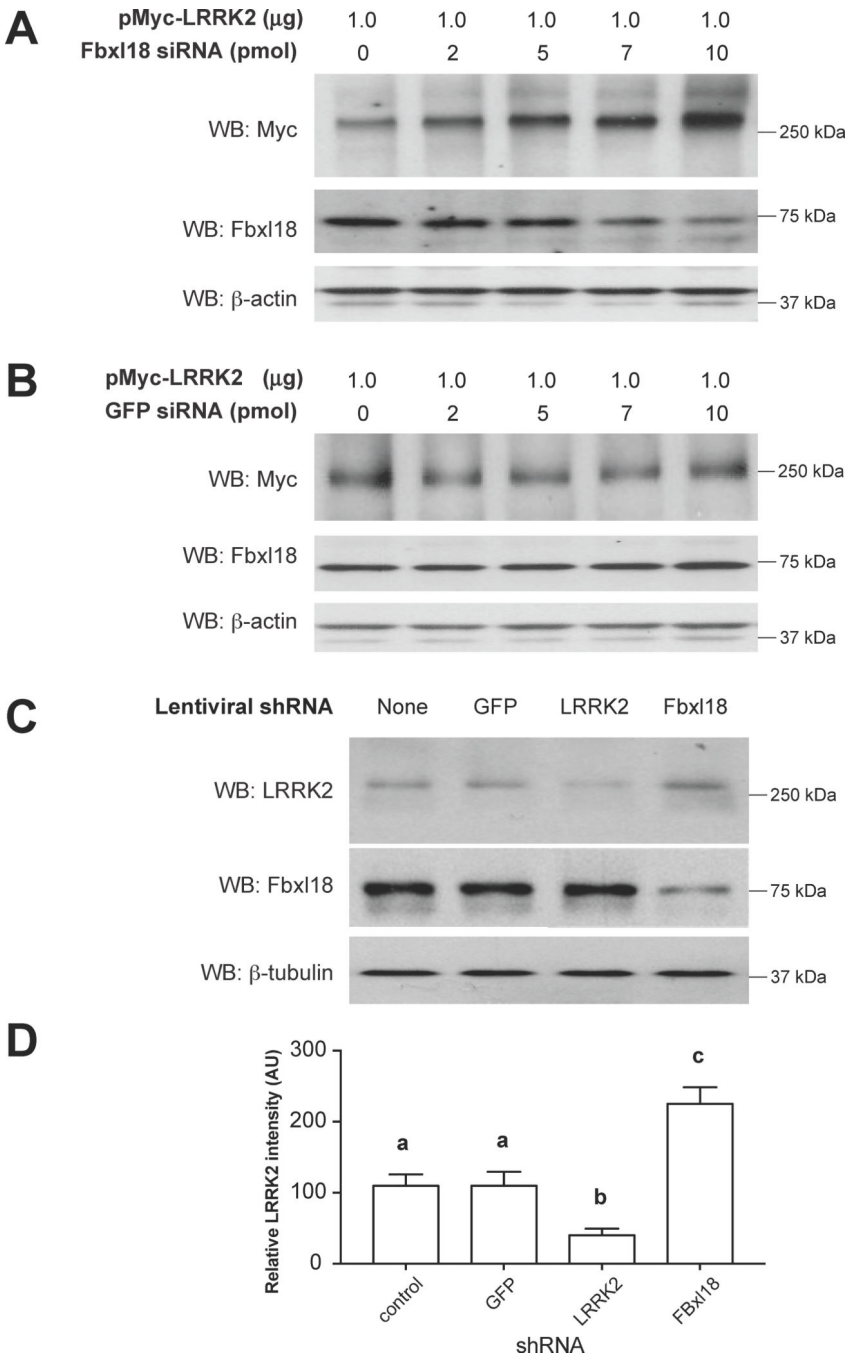

Figure 7.

Knockdown of Fbxl18 attenuates LRRK2 degradation. (A) SH-SY5Y cells were co-transfected with 1.0 μg pMyc-LRRK2 and 0, 2, 5, 7, or 10 pmol of Fbxl18 siRNA. After 48 h, cell lysates were analyzed by western blotting with anti-myc (upper panel), anti-Fbxl18 (middle panel) or anti-β-actin (lower panel). (B) SH-SY5Y cells were co-transfected and analyzed as in (A) except GFP siRNA was used instead of Fbxl18 siRNA. (C) Cultured mouse brain striatal neurons were transduced with GFP, LRRK2 or Fbxl18 shRNA lentiviruses. After 2-day incubation, the endogenous LRRK2 and Fbxl18 levels were

measured by western analysis, using anti-β-tubulin as a loading control for normalization. (D) Densitometry was used to measure LRRK2 levels, which were significantly increased by Fbxl18 shRNA compared to GFP or non-transfected controls. LRRK2 levels (but not Fbxl18 levels) were significantly decreased by LRRK2 shRNA. Bar graph shows mean LRRK2 intensity (N = 3) and error bars show +/− SEM. Columns with the same letter above them are not significantly different whereas columns with different letters are significantly different according to ANOVA followed by Tukey's multiple comparisons test ($p<0.05$).

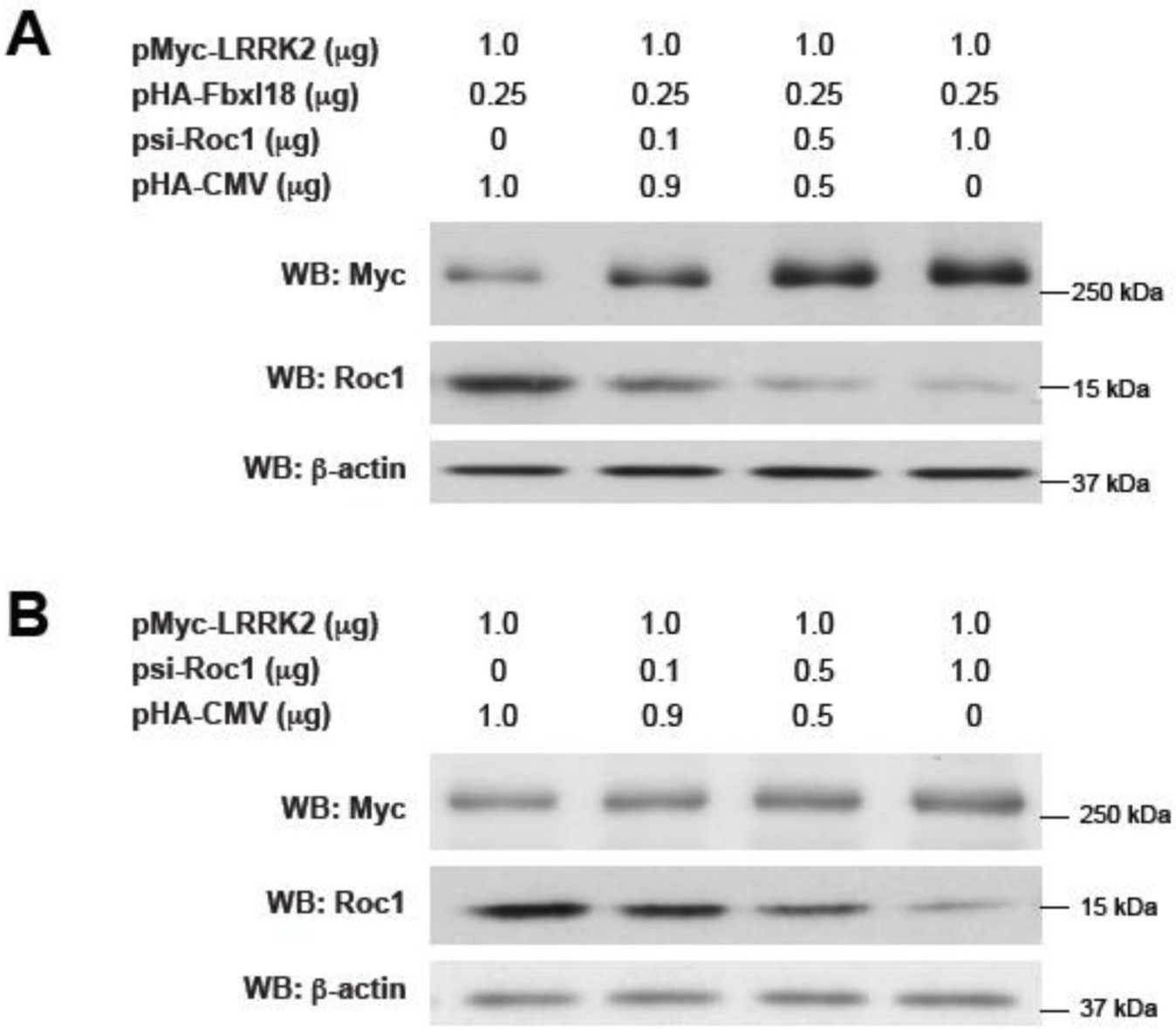

Figure 8.

Roc1 is required for Fbxl18-mediated LRRK2 degradation. (A) HEK293 cells were co-transfected with 1.0 μg of pMyc-LRRK2 and 0.25 μg of pHA-Fbxl18 along with 0, 0.1, 0.5 or 1.0 μg of psi-Roc1 to silence expression of endogenous Roc1. The empty vector pHA-CMV was used to normalize the total amount of DNA for each transfection. After 48 h, cell lysates were analyzed by western blotting with anti-myc, anti-Roc1 and anti-β-actin antibodies. (B) In parallel, cells were co-transfected and analyzed exactly as in (A), except empty vector was used instead of pHA-Fbxl18 expression vector.

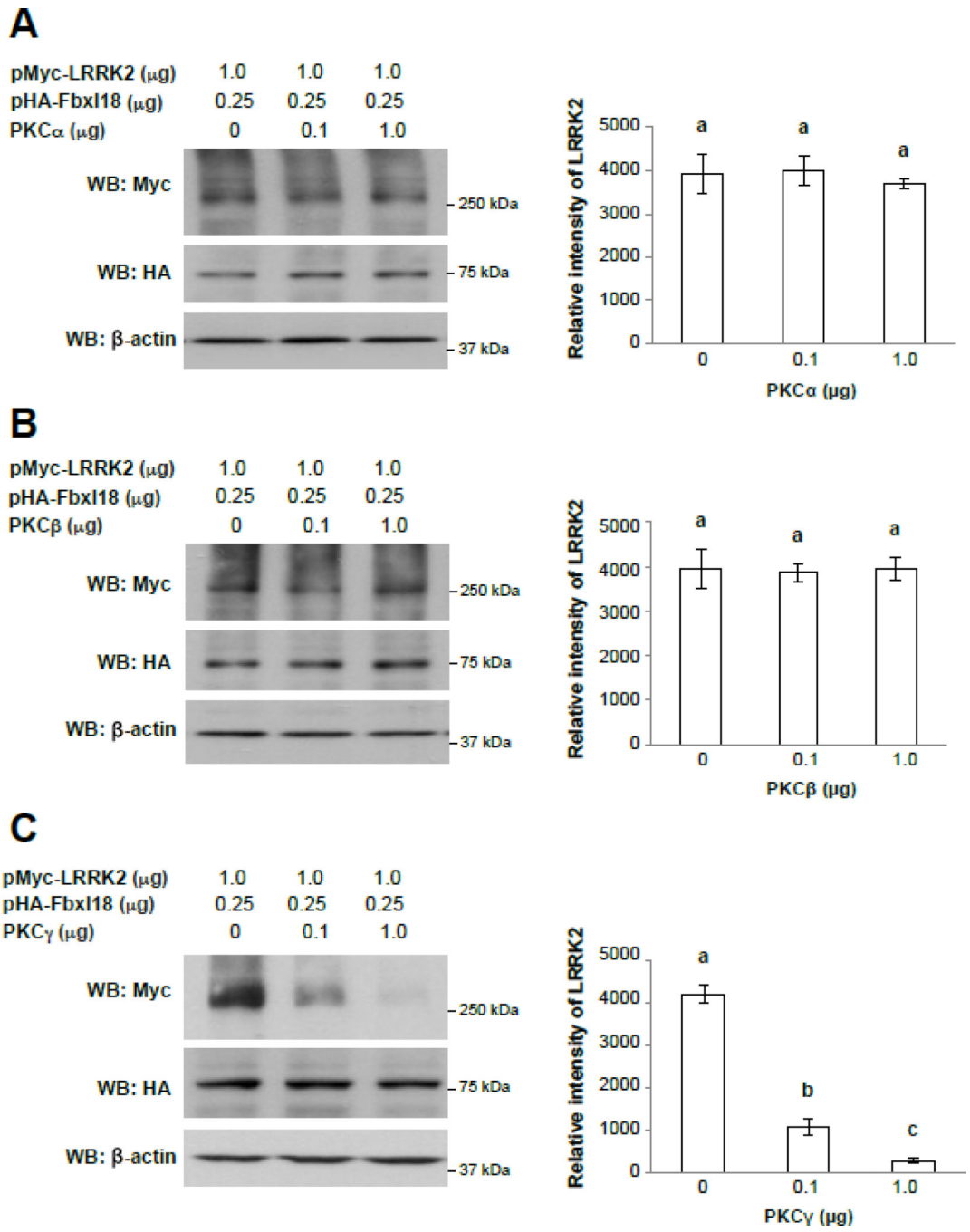

Figure 9.

PKCγ but not PKCα or PKCβ potentiates Fbxl18-mediated degradation of LRRK2. HEK293 cells were co-transfected with fixed amounts of pMyc-LRRK2, pHA-Fbxl18 and increasing amounts of (A) PKCα, (B) PKCβ, or (C) PKCγ. After 48 h, cell lysates were analyzed by western blot using anti-myc, -HA and β-actin antibodies to measure levels of LRRK2, Fbxl18 and β-actin. Bars to the right indicate mean levels of LRRK2 measured by densitometry of myc immunoblots (N = 3) and error bars show +/− SEM. Columns with the same letter above them are not significantly different whereas columns with different letters

are significantly different according to ANOVA followed by Tukey's multiple comparisons test ($p<0.05$).

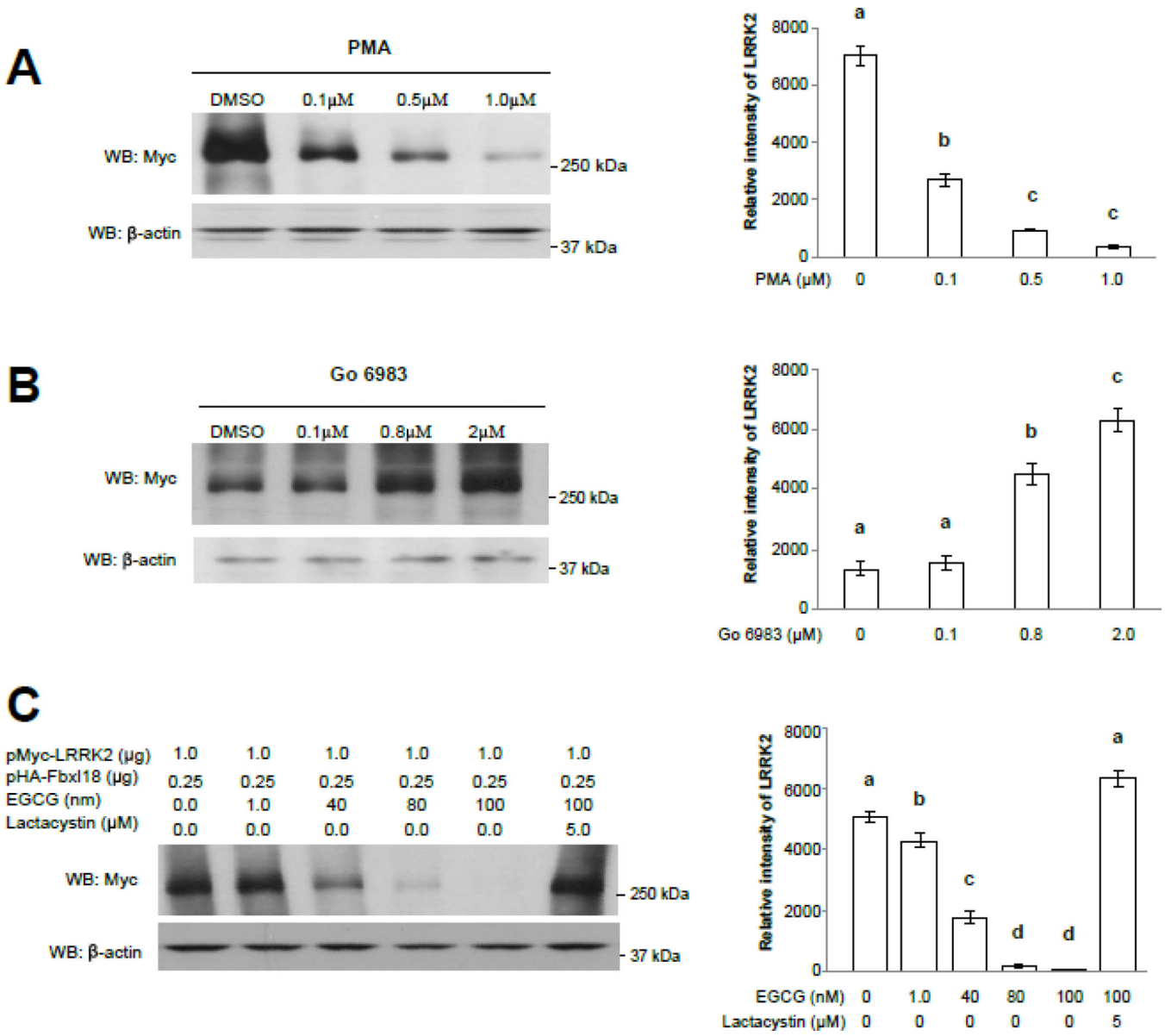

Figure 10.

Activation or inhibition of PKC decreases or increases LRRK2 levels. (A-C) HEK293 cells were co-transfected with pMyc-LRRK2 and pHA-Fbxl18 and treated with the PKC activator PMA (A), the PKC inhibitor Go 6983 (B) or the green tea extract EGCG (C) at the indicated concentrations. Cell lysates were analyzed by anti-myc western blot to measure LRRK2 levels relative to β-actin control. Bar graphs to the right indicate levels of LRRK2 measured by densitometry of myc immunoblots (N = 3) and error bars show +/− SEM. Columns with the same letter above them are not significantly different whereas columns with different letters are significantly different according to ANOVA followed by Tukey's multiple comparisons test ($p<0.05$).

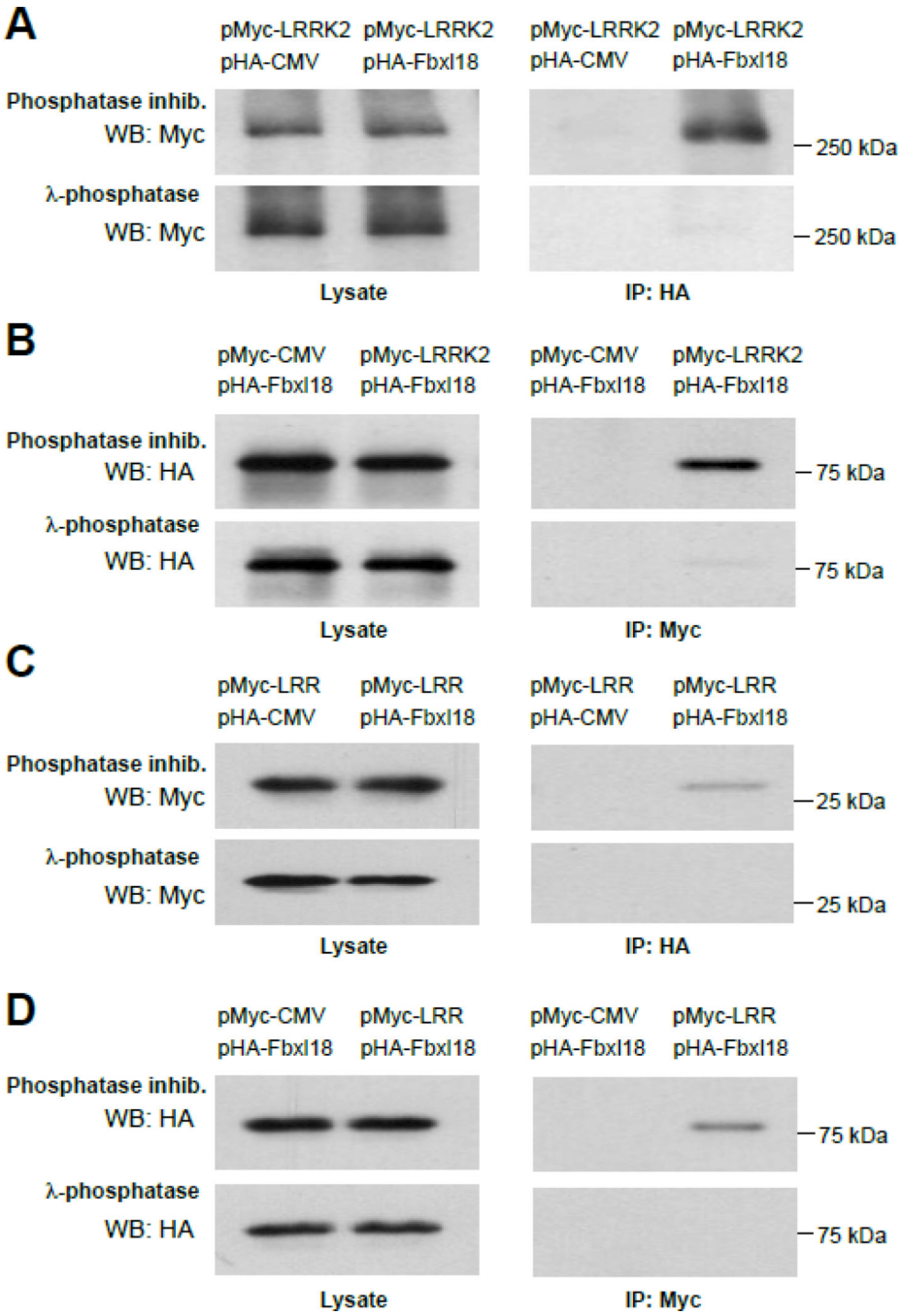

Figure 11.

Treatment of cell lysates with λ-phosphatase abolishes the interaction between Fbxl18 and LRRK2. (A-B) HEK293 cells were co-transfected with the indicated expression vectors for LRRK2 and Fbxl18 together with PKCγ. After 24 h, the cells were lysed in the presence of phosphatase inhibitors to preserve protein phosphorylation or λ-phosphatase to dephosphorylate proteins. Total cell lysates and IPs were analyzed by western blot with HA and myc antibodies as indicated. (C–D) Cells were co-transfected and analyzed as in (A-B) except the LRR domain of LRRK2 was used instead of full-length LRRK2.

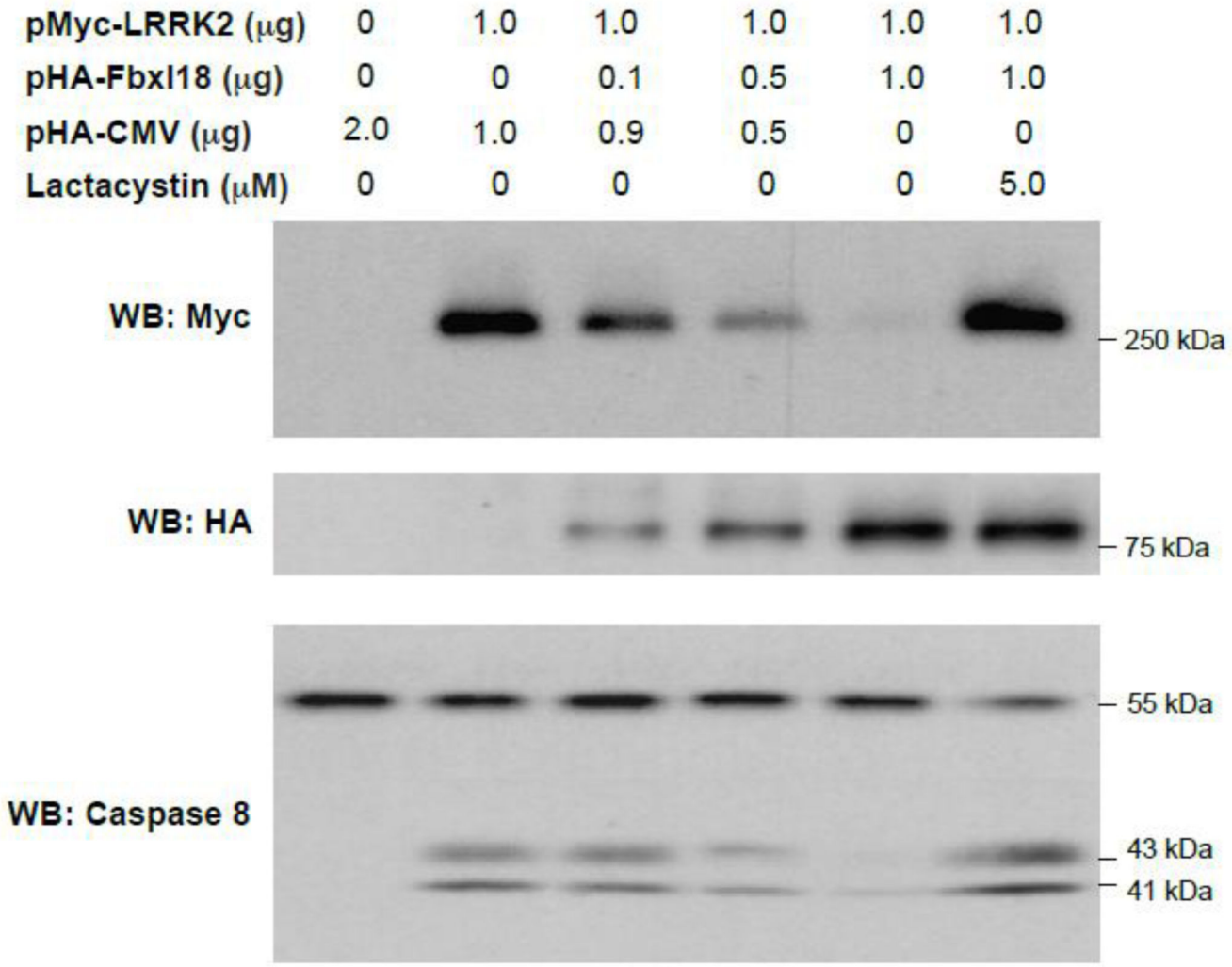

Figure 12.

Fbxl18 inhibits LRRK2-dependent caspase 8 cleavage. SH-SY5Y cells were co-transfected with 1.0 μg of pMyc-LRRK2 and 0, 0.1, 0.5, or 1.0 μg of pHA-Fbxl18. The empty vector pHA-CMV was used to normalize the total amount of DNA for each transfection. The proteasome inhibitor, lactacystin, was added to the cell culture at 0 or 5 μM, as indicated. After 48 h, cell lysates were analyzed by western blotting using anti-myc (upper panel), anti-HA (middle panel) or anti-caspase 8 (lower panel). Full-length caspase 8 appears around 55 kDa and cleaved caspase 8 bands appear at 43 and 41 kDa.

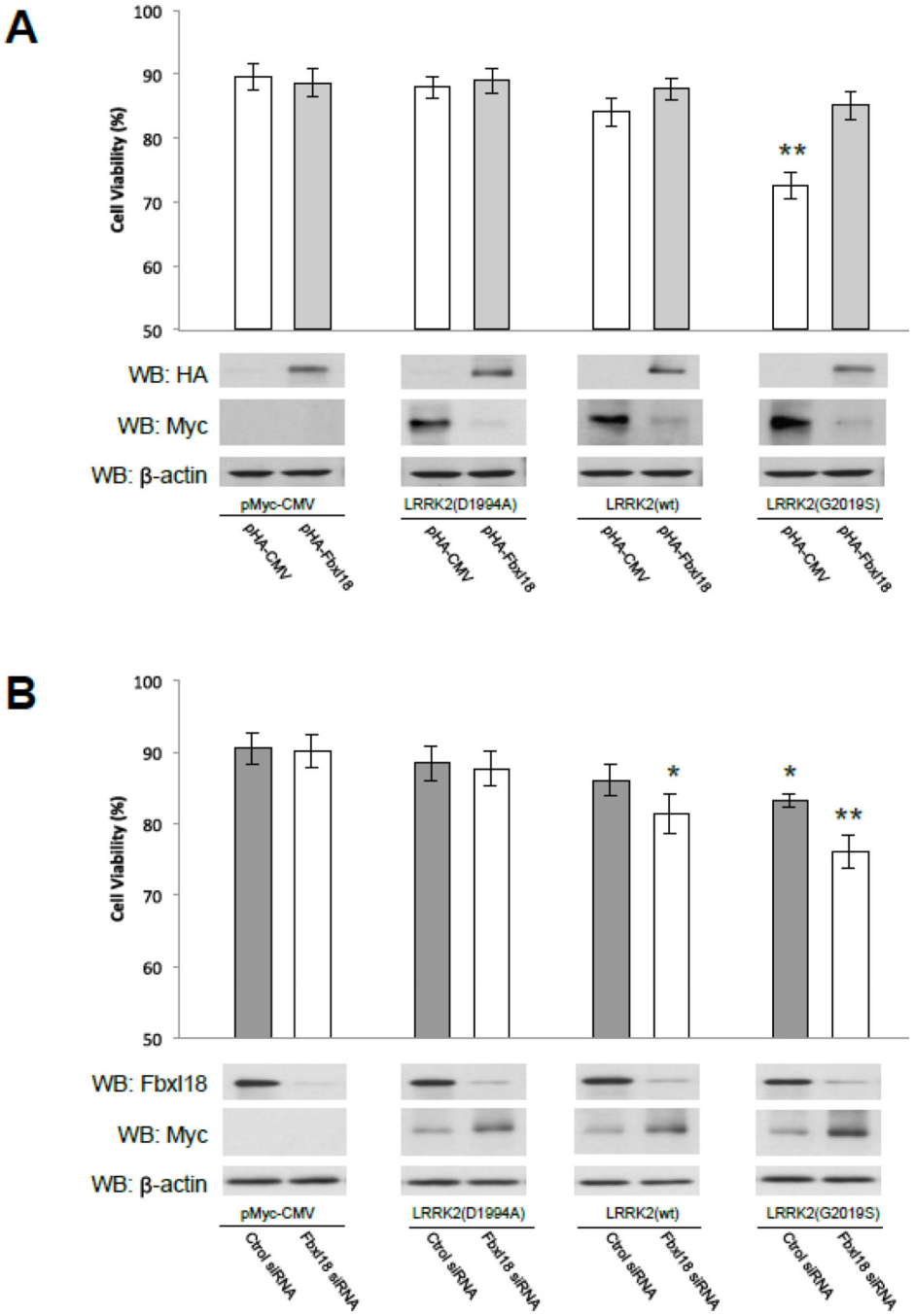

Figure 13.

Increasing or decreasing the level of Fbxl18 respectively mitigates or enhances LRRK2-mediated cell toxicity. (A-B) SH-SY5Y cells were co-transfected with the indicated constructs. After 48 h, cells were labeled with calcein-AM and EthD-1 and the numbers of live and dead cells were counted using an Isocyte automated cell scanner. The bars show mean +/− SEM values from three independent experiments. Below the bars are representative western blots of cell lysates showing protein levels of Fbxl18, LRRK2 and β-

tubulin loading control. * = $p<0.05$ and ** = $p<0.01$ compared to the first lane control (t-test).